Molecular Pharmacology Fast Forward. Published on December 28, 2011 as doi: 10.1124/mol.111.076356
This article has not been copyedited and formatted. The final version may differ from this version.

MOL #76356

An Inducible Cytochrome P450 3A4-dependent Vitamin D Catabolic Pathway

Zhican Wang, Yvonne S. Lin, Xi Emily Zheng, Tauri Senn, Takanori Hashizume, Michele Scian, Leslie J. Dickmann, Sidney D. Nelson, Thomas A. Baillie, Mary F. Hebert, David Blough, Connie L. Davis, Kenneth E. Thummel

Departments of Pharmaceutics (*Z.W, Y.S.L., X.E.Z., T.S., K.E.T.)*, Medicinal Chemistry (*M.S., S.D.N, T.A.B.*), Pharmacy (*M.F.H., D.B.*), and Division of Nephrology (*C.L.D.*), University of Washington, Seattle, WA, USA; Pharmacokinetics Research Laboratories, Dainippon Sumitomo Pharma Co., Ltd, Japan (*T.H.*); Biochemistry and Biophysics Group, Department of Pharmacokinetics and Drug Metabolism, Amgen, Seattle, WA, USA (*L.J.D*).

Molecular Pharmacology Fast Forward. Published on December 28, 2011 as DOI: 10.1124/mol.111.076356
This article has not been copyedited and formatted. The final version may differ from this version.

Running Title Page

Running title: Metabolism of 25-hydroxyvitamin D_3 by CYP3A4

Corresponding author: Kenneth Thummel, Ph.D.

Department of Pharmaceutics, Box 357610

University of Washington

Seattle, WA 98195-7610

Phone: 206-543-0819

FAX: 206-543-3204

Email: thummel@u.washington.edu

Number of text pages: 22

Number of tables: 4

Number of figures: 9

Number of references: 40

Number of words in abstract: 200

Number of words in introduction: 591

Number of words in discussion: 1493

Abbreviations: DBP: vitamin D binding protein; DHB: 6',7'-dihydroxybergamottin; HLM: human liver microsome; KTZ: ketoconazole; LLE: liquid-liquid extraction; MDZ: midazolam; MRM: multiple reaction monitoring; 1α,25$(OH)_2D_3$: 1α,25-dihydroxyvitamin D_3; 1α,25$(OH)_2$-3-epi-D_3: 1α,25-dihydroxy-3-epi-vitamin D_3; 4α,25$(OH)_2D_3$: 4α,25-dihydroxyvitamin D_3; 4β,25$(OH)_2D_3$: 4β,25-dihydroxyvitamin D_3; 23R,25$(OH)_2D_3$: 23R,25-dihydroxyvitamin D_3; 23S,25$(OH)_2D_3$: 23S,25-dihydroxyvitamin D_3; 24R,25$(OH)_2D_3$: 24R,25-dihydroxyvitamin D_3; 24S,25$(OH)_2D_3$: 24R,25-dihydroxyvitamin D_3; 25,26$(OH)_2D_3$: 25,26-dihydroxyvitamin D_3; 1α-OHD_3: 1α-hydroxyvitamin D_3; 25OHD_3: 25-hydroxyvitamin D_3; PTAD: 4-phenyl-1,2,4-triazoline-3,5-dione; PXR: pregnane X receptor; RT: retention time; VDR: vitamin D receptor

Molecular Pharmacology Fast Forward. Published on December 28, 2011 as DOI: 10.1124/mol.111.076356
This article has not been copyedited and formatted. The final version may differ from this version.

Abstract

Vitamin D_3 is critical for the regulation of calcium and phosphate homeostasis. In some individuals, mineral homeostasis can be disrupted by long-term therapy with certain antiepileptic drugs and the antimicrobial agent rifampin, resulting in drug-induced osteomalacia, which is attributed to vitamin D deficiency. We now report a novel CYP3A4-dependent pathway, the 4-hydroxylation of 25-hydroxyvitamin D_3 ($25OHD_3$), the induction of which may contribute to drug-induced vitamin D deficiency. The metabolism of $25OHD_3$ was fully characterized *in vitro*. CYP3A4 was the predominant source of $25OHD_3$ hydroxylation by human liver microsomes, with the formation of $4\beta,25(OH)_2D_3$ dominating (V_{max}/K_m = 1.32 ml/min/nmol enzyme). $4\beta,25(OH)_2D_3$ was found in human plasma at concentrations comparable to that of $1\alpha,25(OH)_2D_3$, and its formation rate in a panel of human liver microsomes was strongly correlated with CYP3A4 content and midazolam hydroxylation activity. Formation of $4\beta,25(OH)_2D_3$ in primary human hepatocytes was induced by rifampin and inhibited by CYP3A4-specific inhibitors. Short-term treatment of healthy volunteers (n = 6) with rifampin selectively induced CYP3A4-dependent $4\beta,25(OH)_2D_3$, but not CYP24A1-dependent $24R,25(OH)_2D_3$ formation, and altered systemic mineral homeostasis. Our results suggest that CYP3A4-dependent $25OHD_3$ metabolism may play an important role in the regulation of vitamin D_3 *in vivo* and in the etiology of drug-induced osteomalacia.

Molecular Pharmacology Fast Forward. Published on December 28, 2011 as DOI: 10.1124/mol.111.076356
This article has not been copyedited and formatted. The final version may differ from this version.

Introduction

Vitamin D_3 is the major source of vitamin D in humans, which is essential for the maintenance of calcium and phosphate homeostasis (DeLuca, 1988; Plum and DeLuca, 2010). Insufficiency or deficiency of vitamin D is a risk factor for metabolic bone diseases such as rickets, osteoporosis and osteomalacia (Holick, 2007; Rosen, 2011; Zhang and Naughton, 2010). Vitamin D_3 is initially converted to 25-hydroxyvitamin D_3 ($25OHD_3$) in the liver; this is considered to be the first step in vitamin D activation (Ohyama and Yamasaki, 2004). $25OHD_3$ is the most abundant circulating form of vitamin D_3 which, under normal conditions, is present at 20 to 50 ng/ml (Plum and DeLuca, 2010; Rosen, 2011). It is the substrate for a second hydroxylase, the mitochondrial cytochrome P450 27B1 (CYP27B1), which is found abundantly in the kidney, resulting in the production of the most biologically active form of vitamin D_3, 1α,25-dihydroxyvitamin D_3 [$1\alpha,25(OH)_2D_3$] (DeLuca, 2008; Sutton and MacDonald, 2003). The biological activities of $1\alpha,25(OH)_2D_3$ are mediated primarily through the vitamin D receptor (VDR), a member of the nuclear superfamily of ligand-activated transcription factors (Pike, 1991). Binding of $1\alpha,25(OH)_2D_3$ to VDR initiates transcriptional cascades leading to the expression of, among others, genes involved in calcium metabolism, cellular proliferation and immune responses (Bouillon et al., 2008; Pike and Meyer, 2010).

Metabolism of $25OHD_3$ at the alkyl side chain is considered to be the critical step in the hormone inactivation pathway. In particular, the carbon centers C-23, C-24, and C-26 are the most susceptible sites for oxidation. Mitochondrial CYP24A1 is recognized as a key enzyme for hydroxylation at either C-23 or C-24 of both $1\alpha,25(OH)_2D_3$ and $25OHD_3$, to give the terminal products of calcitroic acid or a cyclic lactone (Prosser and Jones, 2004; Sakaki et al., 2000). However, Gupta et al. (Gupta et al., 2005; Gupta et al., 2004) reported that CYP3A4 is a

Molecular Pharmacology Fast Forward. Published on December 28, 2011 as DOI: 10.1124/mol.111.076356
This article has not been copyedited and formatted. The final version may differ from this version.

microsomal 25-hydroxylase of vitamin D, exhibiting 24- and 25-hydroxylation activities for 1α-hydroxyvitamin D_3 (1α-OHD_3), 1α-hydroxyvitamin D_2 and vitamin D_2, after screening 16 major human hepatic P450s expressed in baculovirus infected insect cells. In contrast, similar experiments performed by Kamachi et al. (Kamachi et al., 2001) revealed no 25-hydroxylation activity towards 1α-OHD_3 for 14 major P450s including CYP3A4 prepared in β-lymphoblastoid cells. Recently, we reported that CYP3A4 can catalyze the hydroxylation of 1α,25$(OH)_2D_3$ at C-23 and C-24 (Xu et al., 2006). In contrast to CYP24A1 that catalyzes C-23S and C-24R hydroxylation of 1α,25$(OH)_2D_3$, CYP3A4 exhibited an opposite product stereoselectivity, with preferential formation of C-23R- and C-24S-hydroxy products (Sakaki et al., 2000; Xu et al., 2006). Therefore, perturbation of 1α,25$(OH)_2D_3$ elimination through changes in gene expression of these catalytic enzymes can contribute to vitamin D deficiency and emergent disease, as it is thought to be the case for drug-induced osteomalacia (Pack et al., 2004; Pascussi et al., 2005; Xu et al., 2006; Zhou et al., 2006).

Chronic treatment (for at least 2 weeks) with the PXR agonist rifampin results in a marked reduction in 25OHD_3 plasma levels, presumably by enhanced clearance of the hormone (Brodie et al., 1980; Brodie et al., 1982; Shah et al., 1981). This in turn would limit the availability of substrate for the formation of the biologically active 1α,25$(OH)_2D_3$. It is well known that CYP3A4 is induced by certain drugs, such as rifampin via the PXR (Gonzalez, 2007; Zhou, 2008). Thus, induction of *CYP3A4* gene expression by certain drugs may enhance 25OHD_3 catabolism and hence modulate vitamin D_3 effects in the body. Therefore, it was of interest to us to investigate whether CYP3A4 could catalyze the alkyl side chain oxidation of 25OHD_3, as it does with 1α,25$(OH)_2D_3$, leading to vitamin D inactivation. We also examined whether activation of PXR, following treatment with rifampin, could alter the formation of CYP27B1-,

Molecular Pharmacology Fast Forward. Published on December 28, 2011 as DOI: 10.1124/mol.111.076356
This article has not been copyedited and formatted. The final version may differ from this version.

CYP3A4- and CYP24A1-dependent metabolites of $25OHD_3$. The results presented here demonstrate that CYP3A4 is a multi-functional enzyme capable of hydroxylating the alkyl side chain and A-ring of $25OHD_3$ reactions, which might contribute to the regulation of vitamin D_3 metabolism, and that formation of the CYP3A4-dependent, but not the CYP24A1-dependent, products is selectively induced by rifampin in healthy subjects.

Materials and Methods

Materials. 6',7'-dihydroxybergamottin (DHB), EDTA, ketoconazole (KTZ), *n*-butylboronic acid, NADPH, $25OHD_3$, 24R,25-dihydroxyvitamin D_3 [24R,25$(OH)_2D_3$], 4-phenyl-1,2,4-triazoline-3,5-dione (PTAD), sodium periodate, and *N*,*O*-bis(trimethylsilyl)trifluoroacetamide (BSTFA) containing 1% trimethylsilylchlorosilane (TMCS) were purchased from Sigma (St. Louis, MO). 1α,25$(OH)_2D_3$ was purchased from Calbiochem (San Diego, CA). Authentic standards of 23R,25-dihydroxyvitamin D_3 [23R,25$(OH)_2D_3$], 24S,25-dihydroxyvitamin D_3 [24S,25$(OH)_2D_3$] and 25,26-dihydroxyvitamin D_3 [25,26$(OH)_2D_3$] were custom synthesized by SAFC Pharma (Madison WI). 23S,25-Dihydroxyvitamin D_3 [23S,25$(OH)_2D_3$] and 3-epi-1α,25-dihydroxyvitamin D_3 [1α,25$(OH)_2$-3-epi-D_3] were gifts from Dr. Fujishima (Tokushima Bunri University, Japan) and Dr. Sakaki (Toyama Prefectural University, Japan), respectively. Deuterated d_6-$25OHD_3$ and d_6-1α,25$(OH)_2D_3$ (containing six deuterium atoms at C-26 and 27) were purchased from Medical Isotopes Inc. (Pelham, NH). Supersomes containing cDNA-expressed human P450 enzymes and P450 reductase (some with cytochrome b_5) were purchased from BD Gentest (Woburn, MA). Human liver microsomes (HLMs), prepared previously, were generated from the University of Washington School of Pharmacy Human Tissue Bank (Seattle, WA). Basic demographic information and characterization of CYP3A4/5 expression in these

Molecular Pharmacology Fast Forward. Published on December 28, 2011 as DOI: 10.1124/mol.111.076356
This article has not been copyedited and formatted. The final version may differ from this version.

samples has been published previously (Lin et al., 2002). Cryopreserved primary human hepatocytes from three different human liver donors were obtained from either BD Gentest or Invitrogen (Carlsbad, CA).

Characterization of 25OHD$_3$ Metabolism. Due to the light sensitivity of vitamin D, the following procedures were conducted under low light conditions. All 25OHD$_3$ metabolism experiments with recombinant P450 enzymes and HLMs were carried out in 0.1 M potassium phosphate buffer containing 1 mM EDTA at 37 ^{o}C, in a total volume of 0.5 ml. After preincubation of the enzyme with 25OHD$_3$ for 5 min, the reaction was initiated by the addition of 1 mM NADPH. Incubations without NADPH served as negative controls. 25OHD$_3$ was dissolved in methanol, and the total percentage of organic solvent in the incubation volume was 1% for all the incubations.

Reaction kinetic parameters (V_{max} and K_m) for the formation of two major products [4α,25(OH)$_2$D$_3$ and 4β,25(OH)$_2$D$_3$] were determined using 5 pmol of CYP3A4 (co-incubated with P450 reductase and cytochrome b_5) or 50 µg of HLM and 2.5 to 50 µM 25OHD$_3$, incubated for 5 min. These conditions resulted in linear product formation rates at all substrate concentrations tested (data not shown). For screening the various recombinant P450 enzymes for 4-hydroxylation activity, formation rates were determined using 10 pmol of enzyme incubated with 12.5 µM 25OHD$_3$ for 30 min, except for CYP3A4 and CYP3A5 where incubations were conducted for 10 min. After incubation, an aliquot (20 µl) was subjected to liquid-liquid extraction (LLE) and LC-MS/MS analysis. For inhibition studies, we used two CYP3A4 inhibitors, DHB and KTZ. DHB (50 µM) or vehicle was preincubated with CYP3A4 and NADPH for 30 min at 37 ^{o}C before a 65 µl aliquot (with 10 pmol enzyme) was then transferred to a second incubation tube containing 25OHD$_3$. In separate experiments, KTZ (0.5 µM), a

Molecular Pharmacology Fast Forward. Published on December 28, 2011 as DOI: 10.1124/mol.111.076356
This article has not been copyedited and formatted. The final version may differ from this version.

competitive inhibitor, or vehicle was added directly to the incubation mixture before addition of NADPH to initiate reaction. The total volume was 0.5 ml and the final concentrations were 20 nM CYP3A4, 1 mM NADPH and 12.5 µM 25OHD$_3$.

Reactions were terminated with the addition of 0.5 ml ethyl acetate. The vitamin D$_3$ products were then isolated by addition of 5 ml ethyl acetate. After extraction, removal of solvent and reconstitution in mobile phase, the isolated products were analyzed by HPLC with a UV diode array detector. For some experiments, the incubation mixtures were spiked with 2 ng d6-1α,25(OH)$_2$D$_3$ as an internal standard. Following LLE and PTAD derivatization, the derivatized vitamin D$_3$ metabolites were subjected to LC-MS/MS analysis.

HPLC and LC-MS/MS Analysis. Method I: Initial analysis of the *in vitro* 25OHD$_3$ incubation products was performed using an Agilent 1100 series HPLC system (Agilent Technologies, Santa Clara, CA). Chromatographic separation of the major analytes was achieved on a Symmetry C8 (2.1 × 150 mm, 3.5 µm) column (Waters, Milford, WA). The mobile phase consisted of a linear gradient from 70% methanol at 0.25 ml/min as follows: 0 – 40 min, 70% to 80% methanol; 40.1 – 45 min, 90% methanol; 45.1 – 60 min, 70% methanol. An aliquot (5 µl) of reconstituted residue was injected for HPLC-UV analysis and seven authentic vitamin D$_3$ standards were analyzed in parallel. All eight peaks isolated from incubation extracts that eluted between 26 min and 36 min were collected and subjected to periodate cleavage, followed by LC-MS/MS analysis. Method II: LC-MS/MS was performed using an Agilent 1200 series HPLC and an Agilent 6410 triple quadrupole tandem mass spectrometer equipped with an electrospray ionization source, as described previously (Wang et al., 2011). Separation was achieved on a Hypersil Gold (2.1 × 100 mm, 1.9 µm) column (Thermo Scientific). Multiple Reaction Monitoring (MRM) of the transitions *m/z* 574 → 314, 574 → 298, 558 → 298, 564 →

Molecular Pharmacology Fast Forward. Published on December 28, 2011 as DOI: 10.1124/mol.111.076356
This article has not been copyedited and formatted. The final version may differ from this version.

298 and 580 → 314 were employed to detect 1α,25$(OH)_2D_3$, 24R,25$(OH)_2D_3$, 25OHD_3, d_6-25OHD_3 and d_6-1α,25$(OH)_2D_3$, respectively.

Purification of Two Major Metabolites Using HPLC. Vitamin D_3 products from *in vitro* incubations were isolated using LLE, pooled and concentrated under a nitrogen stream. The major vitamin D_3 metabolites were purified by HPLC. The vitamin D_3 metabolites were monitored using UV absorbance at 265 nm. Since multiple metabolites with similar structures were formed, the chromatographic conditions were selected to achieve complete separation of the two major metabolites. Chromatographic isolations were accomplished using an Eclipse XDB-C8 (4.6 × 150 mm, 5 µm) column (Agilent) at a flow rate of 1 ml/min under two different mobile phase conditions. Initially, an isocratic separation (85% methanol: 15% water) was performed and fractions were collected between 4.3 and 5.0 min, which contained the two major unknown metabolites. These fractions were then concentrated under a nitrogen stream and subjected to a second separation using a gradient mobile phase. The proportion of methanol in the mobile phase was as follow: 0 min, 75%; 16 min, 79%; 16.2 to 19 min, 95%; 19.2 to 25 min, 75%. Two major peaks were collected and designated as M1 (RT: 13.4 min) and M2 (14.2 min), which proved to be the isomers of 4,25$(OH)_2D_3$ as defined below.

Structure Identification by GC-MS and ^{1}H-NMR. Gas chromatography-electron impact mass spectrometry (GC-MS) analysis of the trimethylsilyl derivatives of M1 (~0.5 µg) and M2 (~0.8 µg) was carried out using a Shimadzu QP2010 GC-MS (Columbia, MD), as described previously (Xu et al., 2006). Nuclear magnetic resonance (NMR) analysis was accomplished on a Varian Unity-Inova 500 MHz NMR spectrometer. The M1 (~30 µg) and M2 (~15 µg) metabolites were dissolved separately in 0.5 ml of deuteromethanol, and ^{1}H-NMR spectra were acquired at 25 ^{o}C and referenced to residual solvent at 4.87 ppm.

Molecular Pharmacology Fast Forward. Published on December 28, 2011 as DOI: 10.1124/mol.111.076356
This article has not been copyedited and formatted. The final version may differ from this version.

Addition of the 4-Hydroxylated Metabolites into Plasma. After we identified the structures of M1 and M2, the concentrations of these two major metabolites were estimated using their UV absorbance at 265 nm and the calibration curve of $25OHD_3$ plotted as concentration vs. absorbance. An aliquot (50 or 100 pg) of purified M1 or M2 was spiked into 1 ml plasma and then prepared for LC-MS/MS analysis after LLE and derivatization. Additionally, we incubated these plasma extracts with 0.5% sodium periodate to determine the presence of vicinal hydroxyl groups in the vitamin D_3 metabolites as indicated by the disappearance of mass spectral signals for M1 and M2 after periodate cleavage.

Isolation of the 4-Hydroxlated Metabolites from Human Plasma. Isolation of the circulating 4-hydroxylated vitamin D_3 metabolites from human plasma was performed as follows. Outdated plasma (~350 ml) from the Puget Sound Blood Center (Seattle, WA) was divided into 20 portions. After protein precipitation by addition of two volumes of acetonitrile, the supernatants were concentrated by removing acetonitrile under a stream of nitrogen and extracted with an equal volume of methyl tert-butyl ether (MTBE). The organic extracts were combined and concentrated under a nitrogen stream. Since an aqueous component was observed in the residue, three volumes of MTBE were added for a second round of extraction. The organic extracts were then dried under a nitrogen stream, reconstituted in 100 µl methanol and subjected to HPLC-UV analysis. The UV signals of the 4-hydroxylated metabolites, however, were not observed due to interference from signals from other unknown compounds in the extracts. Thus, fractions were collected based on the retention times at which the 4-hydroxylated metabolites were expected to elute. After repeated injections, all fractions putatively containing the metabolites were combined, dried and then subjected to PTAD derivatization. The resulting derivatives were then subjected to LC-MS/MS analysis.

Molecular Pharmacology Fast Forward. Published on December 28, 2011 as DOI: 10.1124/mol.111.076356
This article has not been copyedited and formatted. The final version may differ from this version.

Inter-liver Differences in the Formation of the 4-Hydroxylated Metabolites. In order to evaluate inter-liver differences in the formation of 4α,25$(OH)_2D_3$ and 4β,25$(OH)_2D_3$, we screened a panel of forty-two HLMs, which were prepared as described previously (Lin et al., 2002). The assay was carried out as described above with a 10 min incubation time. The final protein concentration of HLMs was 100 µg/ml, in a total volume of 0.5 ml. After PTAD derivatization and LC-MS/MS analysis, the formation rates of the 4-hydroxylated metabolites were correlated with the previously reported CYP3A4 content (determined by Western blot analysis) or total CYP3A activity (sum of the rates of 1′- and 4-hydroxymidazolam formation from MDZ) (Lin et al., 2002).

Metabolism of 25OHD_3 in Human Hepatocytes. Cryopreserved hepatocytes were thawed at 37 ºC, centrifuged at 100 *g* in cryopreserved hepatocyte recovery medium (CHRM) for 10 min and resuspended in plating media (William's E plus plating supplements: 5% fetal bovine serum, 100 nM dexamethasone, 100 U/ml penicillin and streptomycin, 4 µg/ml insulin, 2 mM GlutaMAX, 15 mM HEPES, pH 7.4). Viability and density were measured by trypan blue exclusion, and 52,000 cells/well were plated onto 96-well collagen I coated plates. Hepatocytes were allowed to attach for 4 to 6 h and then plating media was removed and replaced with maintenance media (DMEM plus maintenance supplements: 100 U/ml penicillin and streptomycin, 6.25 µg/ml insulin, 6.25 µg/mL transferrin, 6.25 ng/ml selenous acid, 1.25 mg/ml bovine serum albumin, 5.35 µg/ml linoleic acid, 2 mM GlutaMAX, 15 mM HEPES, pH 7.4) containing 0.25 mg/ml Matrigel. The following day, cells were treated with rifampin (10 µM, 100 µl/well) or vehicle alone (0.1% DMSO) to elicit induction of CYP3A4. After 48 h treatment, the medium was removed and the cells were washed twice with buffer solution and then preincubated with DHB (20 µM) or vehicle alone (0.2% ethanol) for 4 h. The culture medium

Molecular Pharmacology Fast Forward. Published on December 28, 2011 as DOI: 10.1124/mol.111.076356
This article has not been copyedited and formatted. The final version may differ from this version.

was replaced with fresh medium containing $25OHD_3$ (5 μM) in the presence or absence of DHB (20 μM) for 24 h. At the end of treatment, culture medium (1 ml) was collected and pooled for the quantification of 4-hydroxylated metabolites by LC-MS/MS. Total RNA was isolated using the MagMax 96 RNA Isolation Kit as needed for quantitative reverse transcriptase PCR.

Subject Recruitment. A human pilot study was approved by the University of Washington Human Subjects Review Board and conducted at the University of Washington Medical Center (UWMC). Potential participants (ages 18 to 40 years) were interviewed and provided written informed consent prior to undergoing study procedures. Following a screening evaluation, subjects were excluded from further participation if they had a history or lab tests indicative of liver, kidney, gastrointestinal or heart disease, diabetes, or bone problems; were allergic to rifampin; were taking prescription, over-the-counter or herbal medications; used oral contraceptives or hormone patches; smoked or were pregnant at the time of the study. Eligible subjects were asked to abstain from prescription and over-the-counter medications, herbal products, nutritional supplements, oral contraceptives and grapefruit juice for at least one week prior to and during the study period. They were also requested to abstain from alcohol prior to the first day and during the study period, and to fast for 8-12 hours prior to all study visits.

Study Procedures. Subjects were scheduled for a total of four visits for blood and spot urine collection, all taking place on different days at approximately 9 am. Two visits occurred prior to rifampin administration: Day 0 and on the morning prior to the first rifampin dose, Day 1. Subjects received 600 mg rifampin at 9:00 pm daily with 8 ounces of water, beginning on day 1, for 7 consecutive days. The final two blood and urine collection visits occurred on Day 7 and Day 8. Blood was obtained by venipuncture and serum or plasma was isolated by centrifugation. All biological samples were stored at -80 ^{o}C prior to analysis.

Molecular Pharmacology Fast Forward. Published on December 28, 2011 as DOI: 10.1124/mol.111.076356
This article has not been copyedited and formatted. The final version may differ from this version.

Vitamin D and Biomarker Analysis. The concentrations of 1α,25$(OH)_2D_3$, 24R,25$(OH)_2D_3$, 4β,25$(OH)_2D_3$, and 25OHD_3 in plasma were measured as described previously (Wang et al., 2011). Free and total calcium and inorganic phosphate concentrations in serum, as well as calcium, inorganic phosphate and creatinine concentrations in urine, were all measured using standard clinical laboratory procedures in the Department of Laboratory Medicine at the University of Washington. For each analyte, the average of measurements for Days 0 and 1 (pre-rifampin), and Days 7 and 8 (post-rifampin) is reported.

Statistical Analyses. All kinetic and inhibition experiments with recombinantly expressed enzymes and HLM were performed in triplicate. Resulting data are expressed as the mean ± standard deviation (S.D.) and were compared using one-way ANOVA analysis with Dunnett's or Tukey's multiple comparison tests. An assessment of inter-liver differences in 4α,25$(OH)_2D_3$ and 4β,25$(OH)_2D_3$ formation were obtained from two separate experiments. We used GraphPad Prism (v.5, La Jolla, CA) for the statistical analyses. Statistical comparison of the pre- and post-rifampin treatment measurements were conducted with SAS (Statistical Analysis System). Generalized estimating equations, with treatment period as the independent variable, was employed; a p-value less than 0.05 was considered statistically significant. For regression analysis, sample correlation coefficients and corresponding p-values were calculated; the null hypothesis that the population correlation is zero was tested with a t-test, under the assumption that the population was bivariate normally distributed.

Results

Metabolism of 25OHD_3 by CYP3A4 and HLM. After incubation of 25OHD_3 with CYP3A4 (co-expressed with P450 reductase and cytochrome b_5) or HLM for 90 min, vitamin D_3

Molecular Pharmacology Fast Forward. Published on December 28, 2011 as DOI: 10.1124/mol.111.076356
This article has not been copyedited and formatted. The final version may differ from this version.

products were extracted and subjected to HPLC-UV analysis. The HPLC profiles of 25OHD$_3$ metabolites produced by CYP3A4 and HLMs are depicted in Figure 1A and 1C, respectively. Eight major peaks were detected by UV absorbance, all of which demonstrated the typical vitamin D chromophore (λ_{max} of 265 nm). In order to identify the metabolites by retention time, seven authentic standards with concentrations ranging from 1 to 4 μg/ml were analyzed under the same LC conditions (Figure 1B). To further verify the identity of these metabolites, all eight peaks were collected individually and subjected to periodate cleavage and LC-MS/MS analysis. As summarized in Table 1, nine putative metabolites were identified, seven of which matched the authentic standards by comparison of LC retention times, mass spectra and sensitivity to sodium periodate treatment. Peaks 1 through 4 were identified as 24S,25(OH)$_2$D$_3$, 24R,25(OH)$_2$D$_3$, 23S,25(OH)$_2$D$_3$ and 25,26(OH)$_2$D$_3$, respectively. Peaks 5 and 6, the two major metabolites designated as M1 and M2, were suspected to be unknown dihydroxyvitamin D$_3$ metabolites with two vicinal hydroxyl groups on the A-ring. Peaks 7 and 8 were assigned as mixtures of 23R,25(OH)$_2$D$_3$, 1α,25(OH)$_2$D$_3$ and 1α,25(OH)$_2$-3-epi-D$_3$.

Identification of the Two Major Metabolites. Initially, the two major metabolites, M1 and M2, were thought to be either 2,25(OH)$_2$D$_3$ or 4,25(OH)$_2$D$_3$ regioisomers based on the following criteria: *(i)* both contained two hydroxyl groups on the A-ring, based on a characteristic daughter ion of *m/z* 314 from the PTAD derivative $[M\text{-}H_2O+H]^+$ (*m/z* 574); *(ii)* neither metabolite corresponded to 1α,25(OH)$_2$D$_3$ or 1α,25(OH)$_2$-3-epi-D$_3$ due to their different retention times (Supplemental Figure 1); and *(iii)* both were sensitive to periodate cleavage, although M1 was much more sensitive than M2. In order to fully define the structures, sufficient quantities (> 10 μg) of these two metabolites were purified and characterized by three additional experiments. In the first experiment, the metabolites were converted to the trimethylsilyl ether derivatives and

Molecular Pharmacology Fast Forward. Published on December 28, 2011 as DOI: 10.1124/mol.111.076356
This article has not been copyedited and formatted. The final version may differ from this version.

subjected to GC-MS analysis. As shown in Figure 2, the molecular ions of both M1 and M2 were at *m/z* 632, confirming that they were vitamin D_3 derivatives with three hydroxyl groups. The abundant ion at *m/z* 131 indicated the presence of an OTMS group at C-25. Structurally informative fragment ions were found at *m/z* 503 (M–129) and 413 (M–129–90) for both M1 and M2. The loss of a 129 Da neutral mass from analogous structures has been attributed to the elimination of C-1, C-2 and C-3 together with an OTMS group at C-3 (Araya et al., 2003; Dumaswala et al., 1989). Thus, M1 and M2 are likely to be 4,25$(OH)_2D_3$ isomers. This conclusion was further confirmed by results from a ^{1}H-NMR experiment. As shown in Figure 3, the chemical shifts of the vinylic hydrogens at C-6 of M1 (6.49 ppm) and M2 (6.61 ppm) were shifted downfield, in comparison to the same hydrogens in the spectra of both 25OHD_3 and 1α,25$(OH)_2D_3$, while the chemical shifts of the hydrogen at C-7 of M1 (6.09 ppm) and M2 (6.09 ppm) were similar when compared to the same hydrogen in the standards, 25OHD_3 (6.03 ppm) and 1α,25$(OH)_2D_3$ (6.09 ppm). The downfield shift is most likely the result of an inductive, deshielding field effect of the electronegative hydroxyl group at C-4 on the C-6 proton. Hydroxylation at C-2 would not be expected to have this effect because the hydroxyl group would be too distant from the C-6 proton (Araya et al., 2003). Accordingly, both M1 and M2 were assigned as configurational isomers of 4,25$(OH)_2D_3$. Following a third set of experiments, M1 was identified as 4β,25$(OH)_2D_3$ and M2 as 4α,25$(OH)_2D_3$ due to their differential reactivities with sodium periodate and *n*-butylboronic acid treatment (Xu et al., 2006). Both reactions were predicted to be more facile for adjacent *cis*-dihydroxy groups than *trans*-dihydroxy groups in a cyclic ring system (Alexander et al., 1951). The rate of A-ring cleavage after periodate treatment was much greater for M1 than M2, and only M1 reacted with *n*-butylboronic acid (leading to a loss of $[M+Na]^+$ ion at *m/z* 439 under LC-MS analysis) to generate a product with a $[M+Na]^+$ ion

Molecular Pharmacology Fast Forward. Published on December 28, 2011 as DOI: 10.1124/mol.111.076356
This article has not been copyedited and formatted. The final version may differ from this version.

at *m/z* 505. This result is consistent with the formation of a cyclic boronate, a known product of *cis*- but not *trans*-diols. The larger downfield shift of ~0.12 ppm for the proton at C-6 in the proposed 4α-hydroxy isomer (M2) compared to the 4β-hydroxy isomer (M1) also is consistent with the assignments, since the 4α-hydroxy group will primarily exist in a pseudo-equatorial orientation that is closer to the C-6 hydrogen in M2 than the 4β-hydroxy group in M1 that will primarily exist in a pseudo-axial orientation.

Assessment of 4-Hydroxylation Activity by Various Recombinant P450 Enzymes. In addition to CYP3A4, twelve other recombinantly expressed human P450 enzymes were evaluated for their ability to catalyze the 4-hydroxylation of $25OHD_3$. We found that CYP3A5 (co-incubated with P450 reductase and cytochrome b_5) catalyzed the 4-hydroxylation reaction, whereas the other enzymes had no detectable activity (Table 2). However, the reaction rate for CYP3A5 was ~10% that of CYP3A4 under the same incubation conditions. The metabolism of $25OHD_3$ by CYP24A1 was also studied (incubation performed in Japan by Dr. Sakaki) and as expected, 24R,$25(OH)_2D_3$ was the predominant product and no detectable amount of 4,$25(OH)_2D_3$ was formed (Table 2).

Kinetic Parameters for 4β,$25(OH)_2D_3$ and 4α,$25(OH)_2D_3$ Formation from $25OHD_3$. The kinetics of 4β,$25(OH)_2D_3$ and 4α,$25(OH)_2D_3$ formation were determined using recombinant CYP3A4 and HLM over a range of substrate concentrations (2.5 – 50 μM). The Michaelis-Menten equation was fit to the resulting data, as no evidence for allosterism was observed. As summarized in Table 3, the V_{max} for 4β,$25(OH)_2D_3$ formation was ~2-fold higher than that for 4α,$25(OH)_2D_3$, although the K_m were comparable when determined using either recombinant CYP3A4 or HLMs. The total intrinsic clearance (V_{max}/K_m, sum of 4-hydroxylated metabolites) for CYP3A4 was approximately 1.32 ml/min/nmol.

Molecular Pharmacology Fast Forward. Published on December 28, 2011 as DOI: 10.1124/mol.111.076356
This article has not been copyedited and formatted. The final version may differ from this version.

Inhibition of 25OHD$_3$ 4-Hydroxylation by DHB and KTZ. To further confirm that the 4-hydroxylation of 25OHD$_3$ is catalyzed predominantly by CYP3A4, the effects of a mechanism-based inhibitor DHB and a competitive inhibitor KTZ were evaluated using recombinant CYP3A4 and HLM. The results showed that preincubation with 50 μM DHB for 30 min blocked more than 97% of the 4-hydroxylation activities of both CYP3A4 and HLM (Table 4). Similarly, coincubation of 0.5 μM KTZ with 25OHD$_3$ resulted in > 80% loss of 4-hydroxylation activity. In contrast, DHB did not inhibit the 24-hydroxylation of 25OHD$_3$ by CYP24A1 under similar incubation conditions (data not shown). These results support the conclusion that CYP3A4 is the predominant microsomal enzyme catalyzing 4-hydroxylation of 25OHD$_3$ in human liver.

Metabolism of 25OHD$_3$ in Human Hepatocytes. We also evaluated the contribution of CYP3A4 to the 4-hydroxylation of 25OHD$_3$ in primary human hepatocytes incubated with 5 μM 25OHD$_3$ for 24 h with and without pretreatment with rifampin (10 μM). The *CYP3A4* mRNA level in hepatocytes was significantly increased above baseline by incubation with rifampin for 48 h (rifampin: 43.6 ± 9.5 vs. DMSO: 1.02 ± 0.06). Both 4β,25(OH)$_2$D$_3$ and 4α,25(OH)$_2$D$_3$ metabolites were detected under control (vehicle pretreated) and induced (rifampin pretreated) conditions. On average, 4β,25(OH)$_2$D$_3$ formation compared to 4α,25(OH)$_2$D$_3$ formation was found to be approximately 6-fold higher under control conditions and 9-fold higher under induced conditions (Figure 4). Co-treatment of control and rifampin-pretreated human hepatocytes with DHB resulted in 70% and 81% reductions of 4β,25(OH)$_2$D$_3$ formation, respectively. Interestingly, DHB had no consistent effect on 4α,25(OH)$_2$D$_3$ formation in control cells, but elicited a 30-56% reduction of metabolite formation in rifampin-pretreated cells (Figure 4).

Molecular Pharmacology Fast Forward. Published on December 28, 2011 as DOI: 10.1124/mol.111.076356
This article has not been copyedited and formatted. The final version may differ from this version.

4β,25(OH)$_2$D$_3$ is a Newly Identified Circulating Metabolite in Human Plasma. During the course of developing a sensitive LC-MS/MS assay for the quantification of 1α,25(OH)$_2$D$_3$, an endogenous interfering peak was observed during chromatography of human plasma extracts (Supplemental Figure 2A). Based on its mass spectrum and sensitivity to periodate cleavage, this unknown appeared to be a metabolite of vitamin D$_3$ that bore two hydroxyl groups on the A-ring (Wang et al., 2011). It was hypothesized, therefore, that the interfering peak corresponded to 2,25(OH)$_2$D$_3$ or 4,25(OH)$_2$D$_3$. Two additional experiments described here support the conclusion that this unknown is 4β,25(OH)$_2$D$_3$. As shown in Figure 5A, purified 4β,25(OH)$_2$D$_3$ co-eluted with the unknown, and the intensity of the mass spectrometric signal increased in proportion to the amount of 4β,25(OH)$_2$D$_3$ added to the plasma. In addition, we successfully isolated this compound from 350 ml of human plasma. After LLE and HPLC purification, the isolated fractions from repeated injections were subjected to LC-MS/MS analysis. The ion current chromatograms presented in Figure 5B showed that the material isolated from plasma exhibited identical HPLC and MRM characteristics to those of 4β,25(OH)$_2$D$_3$ purified from the *in vitro* biosynthesis reaction .

Using a novel LC-MS/MS assay, the plasma concentration of 4β,25(OH)$_2$D$_3$ was measured in 25 healthy adult volunteers. As reported previously (Wang et al., 2011), the average concentration of 4β,25(OH)$_2$D$_3$ was ~40 pg/ml, which was comparable to the level of 1α,25(OH)$_2$D$_3$ (60 pg/ml) detected in the same subjects. Interestingly, the levels of 4β,25(OH)$_2$D$_3$ were highly variable among the study population, ranging from 2 to 128 pg/ml, but correlated well with the plasma levels of 25OHD$_3$ (R^2 = 0.73) (Supplemental Figure 3). In agreement with its much lower rate of formation in human hepatocytes, 4α,25(OH)$_2$D$_3$ was detectable in some but not all of the study subjects (data not shown).

Molecular Pharmacology Fast Forward. Published on December 28, 2011 as DOI: 10.1124/mol.111.076356
This article has not been copyedited and formatted. The final version may differ from this version.

Inter-liver Differences in the Formation of 4β,25(OH)$_2$D$_3$ and 4α,25(OH)$_2$D$_3$ from 25OHD$_3$. Since the formation of both 4β,25(OH)$_2$D$_3$ and 4α,25(OH)$_2$D$_3$ from 25OHD$_3$ appear to be catalyzed predominantly by CYP3A4, we investigated whether the formation rates of these metabolites were correlated with CYP3A4 activity or content in livers from different donors. Preparations of HLMs from 42 individual donors were employed, in which the CYP3A4 activity was established using the total MDZ hydroxylation rate and the enzyme content was determined by Western blot analysis (Lin et al., 2002). We incubated this panel of HLMs with 25OHD$_3$ to measure the rates of 4β,25(OH)$_2$D$_3$ and 4α,25(OH)$_2$D$_3$ formation. As shown in Figure 6, the rates of 4β- and 4α-hydroxylation were highly variable, ranging from 1.9 to 204 pmol/min/mg protein and from 0.7 to 93 pmol/min/mg protein, respectively. Both rates were correlated with the total rate of MDZ 1′- and 4-hydroxylation (4β,25(OH)$_2$D$_3$: r^2 = 0.86; 4α,25(OH)$_2$D$_3$: r^2 = 0.83), as well as CYP3A4 protein content (4β,25(OH)$_2$D$_3$: r^2 = 0.59; 4α,25(OH)$_2$D$_3$: r^2 = 0.53). As expected, the rates of 4β- and 4α-hydroxylation were highly correlated with each other (r^2 = 0.99), indicating that the metabolites were being produced by the same enzyme in HLMs.

Induction of 4β,25(OH)$_2$D$_3$ Formation after Oral Doses of Rifampin. We analyzed plasma concentrations of 25OHD$_3$ and three of its primary metabolites: 1α,25(OH)$_2$D$_3$, 24R,25(OH)$_2$D$_3$ and 4β,25(OH)$_2$D$_3$ (Supplemental Figure 2B). Short-term treatment with rifampin for 7 days caused a slight reduction in the concentration of 25OHD$_3$ (-11%, $p < 0.05$), as well as the 24R,25(OH)$_2$D$_3$ level (-13%, $p < 0.05$). Although the average plasma concentration of 1α,25(OH)$_2$D$_3$ also declined with rifampin treatment, the change was not significant. In contrast, there was a significant, nearly 2-fold increase in the plasma concentration of 4β,25(OH)$_2$D$_3$ (Figure 7A). To evaluate the effect of rifampin on the respective 25OHD$_3$ metabolite formation clearances, we calculated the metabolite/parent concentration

Molecular Pharmacology Fast Forward. Published on December 28, 2011 as DOI: 10.1124/mol.111.076356
This article has not been copyedited and formatted. The final version may differ from this version.

ratio for each pathway and compared the individual mean differences. As seen in Figure 7B, an increase in the 4β,25$(OH)_2D_3$/25OHD_3 ratio in all subjects was observed. The ratio change varied between 15–224%, with a mean increase of 120% and the drug effect was highly significant ($p < 0.001$). In contrast, there was no significant change in the metabolite/parent concentration ratio for the 24R,25$(OH)_2D_3$ and 1α,25$(OH)_2D_3$ pathways. Assuming that rifampin does not cause a change in the clearance of the 25OHD_3 metabolites, the data suggest that rifampin caused selective induction of the 4β,25$(OH)_2D_3$ formation clearance pathway, an effect mediated presumably by CYP3A4 induction.

Biomarker Analysis of Mineral Homeostasis. For the same six study subjects, we measured serum intact parathyroid hormone, ionized calcium, total calcium, and phosphate concentrations and urine calcium and phosphate concentrations (normalized for creatinine concentration) before and after rifampin treatment. The majority of these measurements were found within a normal physiological range, which was expected given the health of the subjects and such a short-term treatment with rifampin. However, the results showed important changes after rifampin treatment: all six subjects had decreased serum calcium levels (Figure 8A), four of them had reduced serum phosphate levels with no change in the other two subjects (Figure 8B), four subjects had decreased creatinine-normalized urine calcium (Figure 8C) and five of six subjects had increased creatinine-normalized urine phosphate (Figure 8D). The magnitude of changes in the urine parameters was greater than that of serum parameters. Analyzing the individual pre- versus post rifampin treatment changes, we found that serum calcium levels were significantly decreased (total serum calcium declined by 1.9%; 9.27 vs 9.36 mg/dL, $p = 0.004$) and serum phosphate was reduced by 5% (3.75 vs 3.96 mg/dL, $p = 0.01$). In the urine, the only significant change was urine creatinine-normalized phosphate concentration (UPi/UCr), which

Molecular Pharmacology Fast Forward. Published on December 28, 2011 as DOI: 10.1124/mol.111.076356
This article has not been copyedited and formatted. The final version may differ from this version.

increased by 50% (0.18 vs 0.26, $p = 0.04$). The spot measurements of serum PTH were unchanged by rifampin treatment.

Although there were only six subjects in the study, we observed some inter-individual differences in both vitamin D and mineral homeostasis data. Importantly, we noted that the subject with the smallest increase in 4β,25(OH)$_2$D$_3$ formation also stood out with regard to urinary phosphate excretion (decreased, instead of an increase for the other five subjects; Figure 8). Moreover, the same subject also had the lowest baseline plasma 1α,25(OH)$_2$D$_3$ level and it increased 35% with rifampin treatment (Figure 9A). Overall, there was a significant correlation between the absolute change in plasma 4β,25(OH)$_2$D$_3$ concentration following rifampin treatment and the absolute change in the plasma 1α,25(OH)$_2$D$_3$ concentration ($r = -0.94$, $p < 0.01$) and urinary phosphate excretion ($r = 0.84$, $p < 0.05$) (Figure 9).

Discussion

Metabolism of the major circulating vitamin D$_3$ metabolite, 25OHD$_3$ plays as a key role in vitamin D$_3$ homeostasis. In general, the 1α-hydroxylation of 25OHD$_3$ represents the final activation step, whereas side chain oxidations of 25OHD$_3$ and 1α,25(OH)$_2$D$_3$ by CYP24A1 are the major inactivation pathways (Christakos et al., 2010). Previously, we reported that CYP3A4 also catalyzes 23-/24-hydroxylations of 1α,25(OH)$_2$D$_3$, which provides an alternative pathway for the inactivation of vitamin D$_3$ (Xu et al., 2006). In the present study, we demonstrated that CYP3A4 also catalyzes 25OHD$_3$ metabolism and produces nine mono-hydroxylated metabolites *in vitro* (Figure 10). Seven minor metabolites were identified by comparison with authentic standards; these included the 23-, 24- and 26-hydroxy products of the alkyl side chain. Production of these minor hydroxylated products of 25OHD$_3$ [23R,25(OH)$_2$D$_3$, 23S,25(OH)$_2$D$_3$,

Molecular Pharmacology Fast Forward. Published on December 28, 2011 as DOI: 10.1124/mol.111.076356
This article has not been copyedited and formatted. The final version may differ from this version.

24R,25$(OH)_2D_3$, 24S,25$(OH)_2D_3$, and 25,26$(OH)_2D_3$] by CYP3A4 is consistent with previous reports demonstrating that CYP3A4 can oxidize the vitamin D_3 core structure at C-23, C-24 and C-26 positions (Xu et al., 2006). Although the relative efficiency of their formation was very low, formation of 1α,25$(OH)_2D_3$ identified in this study could possibly represent an alternative paracrine activation pathway because of the large abundance of CYP3A4 in liver and small intestine. Recent studies indicate that CYP27B1 can be expressed extra-renally in many normal tissues and under pathologic situations, and therefore could be responsible for the extra-renal formation of 1α,25$(OH)_2D_3$ (Hewison et al., 2007; Hewison et al., 2000). However, it cannot be excluded that CYP3A4 might contribute to the formation of 1α,25$(OH)_2D_3$ as well, particularly in tissues where CYP3A4 is highly expressed.

The two major metabolites of 25OHD_3 produced by CYP3A4 were 4β,25$(OH)_2D_3$ and 4α,25$(OH)_2D_3$, and CYP3A4 is the dominant source of these A-ring hydroxylated products in human liver. This is supported by the fact that both 4β,25$(OH)_2D_3$ and 4α,25$(OH)_2D_3$ were generated by recombinant CYP3A4 and HLMs. Moreover, the HLM reaction was inhibited substantially by addition of the selective CYP3A4 inhibitors DHB and KTZ. When other microsomal P450s were screened, only CYP3A5 catalyzed the 4-hydroxylation reactions, though the formation rates for CYP3A5 were much lower than those for CYP3A4. Using HLMs isolated from 42 different liver tissues, we determined that the formation rates of 4β,25$(OH)_2D_3$ and 4α,25$(OH)_2D_3$ were well correlated with CYP3A4 MDZ hydroxylation and protein expression.

In contrast, we found that the mitochondrial enzyme, CYP24A1, lacked any detectable 4-hydroxylase activity. Incubation of primary human hepatocytes with DHB, a CYP3A4 selective, mechanism-based inhibitor, effectively inhibited the 4β-hydroxylation reaction, indicating the

Molecular Pharmacology Fast Forward. Published on December 28, 2011 as DOI: 10.1124/mol.111.076356
This article has not been copyedited and formatted. The final version may differ from this version.

absence of any other appreciable source of 4β,25$(OH)_2D_3$ formation. However, there was a discrepancy between microsomal and hepatocyte 4α,25$(OH)_2D_3$ formation with regard to the inhibitory effect of DHB. The CYP3A4 inhibitor decreased 4α,25$(OH)_2D_3$ formation in HLMs, but was less effective in human hepatocytes under basal conditions, although the inhibitory effect was seen after rifampin induction. We do not have an explanation for the discrepancy, but note that the relative formation of the 4α-metabolite in hepatocytes was much less than that predicted by recombinant enzyme and microsomal activities. It is possible that most of the metabolite, once formed by CYP3A4, is rapidly cleared by another metabolic pathway (i.e., sequential oxidation or conjugation) and that the residual amounts detected in the control hepatocyte incubations do not derive from CYP3A4. Similarly in human plasma, 4α,25$(OH)_2D_3$ was detectable in some but not all of the study subjects, and its level was relatively low.

4β,25$(OH)_2D_3$ was also identified as an endogenous circulating metabolite in human plasma. Due to its structural similarity to 1α,25$(OH)_2D_3$, a new LC-MS/MS method was developed to chromatographically separate and quantitate 4β,25$(OH)_2D_3$, 4α,25$(OH)_2D_3$ and 1α,25$(OH)_2D_3$ (Wang et al., 2011). In 25 healthy subjects, the mean levels of 4β,25$(OH)_2D_3$ (40 pg/ml) were comparable to that of 1α,25$(OH)_2D_3$ (60 pg/ml), but much less than those of 25OHD_3 (25.6 ng/ml) and 24R,25$(OH)_2D_3$ (2.3 ng/ml). Although correlated with each other, the ratio of 4β,25$(OH)_2D_3$ to 25OHD_3 was still variable, possibly due to differing *in vivo* CYP3A4 activities in each subject. Indeed, we observed significant inter-individual difference in 4β,25$(OH)_2D_3$ formation using HLMs prepared from different liver donors. Thus, it is possible that 4β,25$(OH)_2D_3$ might be an endogenous biomarker for systemic CYP3A4 activity, which remains to be explored.

Molecular Pharmacology Fast Forward. Published on December 28, 2011 as DOI: 10.1124/mol.111.076356
This article has not been copyedited and formatted. The final version may differ from this version.

Although a novel finding, the production of A-ring hydroxylated metabolites from $25OHD_3$ by CYP3A4 is not surprising. Thierry-Palmer et al. (Thierry-Palmer et al., 1988) reported that $25OHD_3$ was hydroxylated at the C-2 or C-4 position by rat renal microsomes *in vitro*, because the product was sensitive to periodate cleavage. Rao et al. (Rao et al., 1999) isolated and identified a similar vitamin D_2 metabolite, $4,25(OH)_2D_2$ from serum in vitamin D_2-intoxicated rats. In addition, Takeda et al. reported that $2\alpha,25(OH)_2D_3$ was produced from microbial hydroxylation of vitamin D_3 by *P. autotrophica* (Takeda et al., 2006). Finally, Araya et al. (Araya et al., 2003) recently reported that $4\beta,25(OH)_2D_3$ was produced *in vitro* by recombinant human CYP27A1, a hepatic mitochondrial vitamin D_3 25-hydroxylase. However, the maximal rate of conversion of $25OHD_3$ to $4\beta,25(OH)_2D_3$ by CYP27A1 (0.024 pmol/min/pmol) was much lower than what we observed for CYP3A4 in the present study (6.4 pmol/min/pmol). This does not necessarily equate to a difference in the formation clearance, but we found that DHB pretreatment of human hepatocytes greatly diminished the 4β-hydroxylation reaction, demonstrating the dominance of CYP3A4 in the metabolic process. It remains to be determined whether the CYP3A4 catalyzed 4-hydroxylation reaction contributes significantly to the clearance of $25OHD_3$ *in vivo*. However, the formation clearance of $4\beta,25(OH)_2D_3$ by CYP3A4 is considerable and although circulating levels of $4\beta,25(OH)_2D_3$ are far less than those of $24R,25(OH)_2D_3$, this difference could be the result of a much more rapid clearance of $4\beta,25(OH)_2D_3$ than $24R,25(OH)_2D_3$, rather than a more efficient formation of $24R,25(OH)_2D_3$.

Long-term treatment with certain drugs, e.g. rifamycins and barbiturates, has been associated with altered bone metabolism and decreased bone density (Pack et al., 2004; Shah et al., 1981). The adverse effect has been attributed to a dysregulation of vitamin D homeostasis and the transcription of some of the genes that it controls (e.g., intestinal TRPV6), principally through a

Molecular Pharmacology Fast Forward. Published on December 28, 2011 as DOI: 10.1124/mol.111.076356
This article has not been copyedited and formatted. The final version may differ from this version.

drug-induced enhancement of $25OHD_3$ and/or $1\alpha,25(OH)_3D_3$ catabolic clearance (Pascussi et al., 2005; Xu et al., 2006; Zhou et al., 2006). Results from our pilot study showed that short-term rifampin treatment selectively induced CYP3A4-dependent $4\beta,25(OH)_2D_3$ formation, while having no appreciable effect on the CYP24A1- and CYP27B1-catalyzed pathways of $25OHD_3$ elimination. Moreover, we observed a decline in the absolute plasma $25OHD_3$ level with short-term rifampin treatment, which is consistent with the more pronounced reduction in hormone level seen with a longer (2-week) duration of rifampin treatment (Brodie et al., 1980; Brodie et al., 1982). In addition, the short duration of rifampin treatment (7 days) was associated with significant changes in the renal excretion of inorganic phosphate, as well as plasma calcium and phosphate concentrations, suggesting the possibility of a significant reduction in the absorption of calcium as a result of enhanced intestinal vitamin D metabolism.

There are several caveats to our interpretation of the clinical study results beyond the relative small subject number. First, the dietary intake of calcium and phosphate was uncontrolled, potentially introducing inter-day dietary noise to the biochemical measurements. In addition, we used creatinine-normalized calcium and phosphate measurements from spot urine samples as an approximation of the 24-hour calcium and phosphate excretion rates. This introduces uncertainties about intra-day variation (Gokce et al., 1991; Topal et al., 2008). It is also possible that longer term (i.e., chronic) treatment with rifampin could produce different effects, in particular the $24R,25(OH)_2D_3$ metabolite if it has a plasma half-life much longer than seven days. These limitations can be easily addressed in a longer duration, prospective investigation, with a sample size powered based on the mean effects and variation observed in the current pilot study.

We also note that the enhancement of vitamin D clearance by drugs such as rifampin, and

Molecular Pharmacology Fast Forward. Published on December 28, 2011 as DOI: 10.1124/mol.111.076356
This article has not been copyedited and formatted. The final version may differ from this version.

increased risk of drug-induced osteomalacia, has been attributed to a PXR-mediated activation of *CYP24A1* gene transcription (Pascussi et al., 2005). However, we have previously suggested that activation of *CYP3A4* transcription represents an alternative or complementary mechanism behind the adverse effect (Xu et al., 2006; Zhou et al., 2006). Results from the current investigation support the hypothesis that it is CYP3A4 induction and enhanced 4β,25$(OH)_2D_3$ formation, and not CYP24A1 induction and enhanced 24R,25$(OH)_2D_3$ formation, that contributes to the reduction in 25OHD_3 levels following chronic treatment with PXR agonists and increases the risk of osteomalacia.

In summary, CYP3A4 is able to catalyze 25OHD_3 hydroxylation at multiple positions. One of the major products, 4β,25$(OH)_2D_3$, a newly identified circulating metabolite, is produced predominantly by CYP3A4 in human liver and might be an endogenous biomarker for assessment of CYP3A4 activity *in vivo*. In addition, short-term treatment with the PXR agonist rifampin selectively induced CYP3A4-dependent 4β,25$(OH)_2D_3$ formation and altered systemic mineral homeostasis *in vivo*. These changes may underlie the increased risk of osteomalacia associated with chronic administration of rifampin and other PXR agonists. Whether the 4β/α-hydroxy metabolites possess biological activities, as do other A-ring oxidized metabolites, remains to be explored.

Molecular Pharmacology Fast Forward. Published on December 28, 2011 as DOI: 10.1124/mol.111.076356
This article has not been copyedited and formatted. The final version may differ from this version.

Acknowledgments

We thank Dr. Toshie Fujishima (Tokushima Bunri University, Japan) for the gift of 23S,25$(OH)_2D_3$, and Dr. Toshiyuki Sakaki (Toyama Prefectural University, Japan) for the gift of 1α,25$(OH)_2$-3-epi-D_3 and incubation of 25OHD_3 with CYP24A1. The authors would also like to thank Michelle Doyle for her assistance in the conduct of the clinical study.

Molecular Pharmacology Fast Forward. Published on December 28, 2011 as DOI: 10.1124/mol.111.076356
This article has not been copyedited and formatted. The final version may differ from this version.

Authorship Contributions

Participated in research design: Wang, Lin, Zheng, Hebert, Davis, Thummel

Conducted experiments: Wang, Lin, Zheng, Senn, Hashizume, Scian, Davis, Dickmann,

Contributed new reagents or analytical tools: Wang, Lin, Senn

Performed data analysis: Wang, Lin, Zheng, Senn, Hashizume, Scian, Dickmann, Nelson, Baillie, Blough, Thummel

Wrote or contributed to the writing of the manuscript: Wang, Lin, Nelson, Baillie, Hebert, Blough, Thummel

References

Alexander BH, Dimler RJ and Mehltretter CL (1951) D-Galactosan(1,4)α(1,6): Its Structure and Resistance to Periodate Oxidation. *J Am Chem Soc* **73**(10):4658-4659.

Araya Z, Hosseinpour F, Bodin K and Wikvall K (2003) Metabolism of 25-hydroxyvitamin D3 by microsomal and mitochondrial vitamin D3 25-hydroxylases (CYP2D25 and CYP27A1): a novel reaction by CYP27A1. *Biochim Biophys Acta* **1632**(1-3):40-47.

Bouillon R, Carmeliet G, Verlinden L, van Etten E, Verstuyf A, Luderer HF, Lieben L, Mathieu C and Demay M (2008) Vitamin D and human health: lessons from vitamin D receptor null mice. *Endocr Rev* **29**(6):726-776.

Brodie MJ, Boobis AR, Dollery CT, Hillyard CJ, Brown DJ, MacIntyre I and Park BK (1980) Rifampicin and vitamin D metabolism. *Clin Pharmacol Ther* **27**(6):810-814.

Brodie MJ, Boobis AR, Hillyard CJ, Abeyasekera G, Stevenson JC, MacIntyre I and Park BK (1982) Effect of rifampicin and isoniazid on vitamin D metabolism. *Clin Pharmacol Ther* **32**(4):525-530.

Christakos S, Ajibade DV, Dhawan P, Fechner AJ and Mady LJ (2010) Vitamin D: Metabolism. *Endocrinol Metab Clin North Am* **39**(2):243-253.

DeLuca HF (1988) The vitamin D story: a collaborative effort of basic science and clinical medicine. *The FASEB Journal* **2**(3):224-236.

DeLuca HF (2008) Evolution of our understanding of vitamin D. *Nutr Rev* **66**(10 Suppl 2):S73-87.

Dumaswala R, Setchell KD, Zimmer-Nechemias L, Iida T, Goto J and Nambara T (1989) Identification of 3 alpha,4 beta,7 alpha-trihydroxy-5 beta-cholanoic acid in human bile:

reflection of a new pathway in bile acid metabolism in humans. *J Lipid Res* **30**(6):847-856.

Eguchi T and Ikekawa N (1990) Conformational analysis of 1α,25-dihydroxyvitamin D3 by nuclear magnetic resonance. *Bioorg Chem* **18**(1):19-29.

Gokce C, Gokce O, Baydinc C, Ilhan N, Alasehirli E, Ozkucuk F, Tasci M, Atikeler MK, Celebi H and Arslan N (1991) Use of Random Urine Samples to Estimate Total Urinary Calcium and Phosphate Excretion. *Arch Intern Med* **151**(8):1587-1588.

Gonzalez FJ (2007) CYP3A4 and pregnane X receptor humanized mice. *J Biochem Mol Toxicol* **21**(4):158-162.

Gupta RP, He YA, Patrick KS, Halpert JR and Bell NH (2005) CYP3A4 is a vitamin D-24- and 25-hydroxylase: analysis of structure function by site-directed mutagenesis. *J Clin Endocrinol Metab* **90**(2):1210-1219.

Gupta RP, Hollis BW, Patel SB, Patrick KS and Bell NH (2004) CYP3A4 is a human microsomal vitamin D 25-hydroxylase. *J Bone Miner Res* **19**(4):680-688.

Hewison M, Burke F, Evans KN, Lammas DA, Sansom DM, Liu P, Modlin RL and Adams JS (2007) Extra-renal 25-hydroxyvitamin D3-1alpha-hydroxylase in human health and disease. *J Steroid Biochem Mol Biol* **103**(3-5):316-321.

Hewison M, Zehnder D, Bland R and Stewart PM (2000) 1alpha-Hydroxylase and the action of vitamin D. *J Mol Endocrinol* **25**(2):141-148.

Holick MF (2007) Vitamin D deficiency. *N Engl J Med* **357**(3):266-281.

Kamachi S, Sugimoto K, Yamasaki T, Hirose N, Ide H and Ohyama Y (2001) Metabolic activation of 1alpha-hydroxyvitamin D3 in human liver microsomes. *Xenobiotica* **31**(10):701-712.

Kamao M, Tatematsu S, Hatakeyama S, Sakaki T, Sawada N, Inouye K, Ozono K, Kubodera N, Reddy GS and Okano T (2004) C-3 epimerization of vitamin D3 metabolites and further metabolism of C-3 epimers: 25-hydroxyvitamin D3 is metabolized to 3-epi-25-hydroxyvitamin D3 and subsequently metabolized through C-1alpha or C-24 hydroxylation. *J Biol Chem* **279**(16):15897-15907.

Lin YS, Dowling ALS, Quigley SD, Farin FM, Zhang J, Lamba J, Schuetz EG and Thummel KE (2002) Co-regulation of CYP3A4 and CYP3A5 and contribution to hepatic and intestinal midazolam metabolism. *Mol Pharmacol* **62**(1):162-172.

Ohyama Y and Yamasaki T (2004) Eight cytochrome P450s catalyze vitamin D metabolism. *Front Biosci* **9**:3007-3018.

Pack AM, Gidal B and Vazquez B (2004) Bone disease associated with antiepileptic drugs. *Cleve Clin J Med* **71 Suppl 2**:S42-48.

Pascussi JM, Robert A, Nguyen M, Walrant-Debray O, Garabedian M, Martin P, Pineau T, Saric J, Navarro F, Maurel P and Vilarem MJ (2005) Possible involvement of pregnane X receptor-enhanced CYP24 expression in drug-induced osteomalacia. *J Clin Invest* **115**(1):177-186.

Pike JW (1991) Vitamin D_3 receptors: structure and function in transcription. *Annu Rev Nutr* **11**:189-216.

Pike JW and Meyer MB (2010) The vitamin D receptor: new paradigms for the regulation of gene expression by 1,25-dihydroxyvitamin D_3. *Endocrinol Metab Clin North Am* **39**(2):255-269.

Plum LA and DeLuca HF (2010) Vitamin D, disease and therapeutic opportunities. *Nat Rev Drug Discov* **9**(12):941-955.

Prosser DE and Jones G (2004) Enzymes involved in the activation and inactivation of vitamin D. *Trends Biochem Sci* **29**(12):664-673.

Rao DS, Dayal R, Siu-Caldera ML, Horst RL, Uskokovic MR, Tserng KY and Reddy GS (1999) Isolation and identification of 4,25-dihydroxyvitamin D_2: a novel A-ring hydroxylated metabolite of vitamin D2. *J Steroid Biochem Mol Biol* **71**(1-2):63-70.

Rosen CJ (2011) Clinical practice. Vitamin D insufficiency. *N Engl J Med* **364**(3):248-254.

Sakaki T, Sawada N, Komai K, Shiozawa S, Yamada S, Yamamoto K, Ohyama Y and Inouye K (2000) Dual metabolic pathway of 25-hydroxyvitamin D_3 catalyzed by human CYP24. *Eur J Biochem* **267**(20):6158-6165.

Shah SC, Sharma RK, Hemangini and Chitle AR (1981) Rifampicin induced osteomalacia. *Tubercle* **62**(3):207-209.

Sutton AL and MacDonald PN (2003) Vitamin D: more than a "bone-a-fide" hormone. *Mol Endocrinol* **17**(5):777-791.

Takeda K, Kominato K, Sugita A, Iwasaki Y, Shimazaki M and Shimizu M (2006) Isolation and identification of 2alpha,25-dihydroxyvitamin D3, a new metabolite from Pseudonocardia autotrophica 100U-19 cells incubated with Vitamin D3. *Steroids* **71**(8):736-744.

Thierry-Palmer M, Gray TK and Napoli JL (1988) Ring hydroxylation of 25-hydroxycholecalciferol by rat renal microsomes. *J Steroid Biochem* **29**(6):623-628.

Topal C, Algun E, Sayarlioglu H, Erkoc R, Soyoral Y, Dogan E, Sekeroglu R and Cekici S (2008) Diurnal rhythm of urinary calcium excretion in adults. *Ren Fail* **30**(5):499-501.

Wang Z, Senn T, Kalhorn T, Zheng XE, Zheng S, Davis CL, Hebert MF, Lin YS and Thummel KE (2011) Simultaneous measurement of plasma vitamin D(3) metabolites, including

4beta,25-dihydroxyvitamin D(3), using liquid chromatography-tandem mass spectrometry. *Anal Biochem* **418**(1):126-133.

Xu Y, Hashizume T, Shuhart MC, Davis CL, Nelson WL, Sakaki T, Kalhorn TF, Watkins PB, Schuetz EG and Thummel KE (2006) Intestinal and hepatic CYP3A4 catalyze hydroxylation of 1α,25-dihydroxyvitamin D_3: implications for drug-induced osteomalacia. *Mol Pharmacol* **69**(1):56-65.

Zhang R and Naughton DP (2010) Vitamin D in health and disease: current perspectives. *Nutr J* **9**:65.

Zhou C, Assem M, Tay JC, Watkins PB, Blumberg B, Schuetz EG and Thummel KE (2006) Steroid and xenobiotic receptor and vitamin D receptor crosstalk mediates CYP24 expression and drug-induced osteomalacia. *J Clin Invest* **116**(6):1703-1712.

Zhou SF (2008) Drugs behave as substrates, inhibitors and inducers of human cytochrome P450 3A4. *Curr Drug Metab* **9**(4):310-322.

Footnotes

This work was supported by the National Institutes of Health grants [R01GM063666], [P01GM032165], [P30ES07033] and [UL1RR025014].

Xi Emily Zheng's present address is: Nassau University Medical Center, 2201 Hempstead Turnpike, East Meadow, NY 11554

Legends for figures

Figure 1. HPLC profiles of the vitamin D metabolites produced from $25OHD_3$ by incubation with recombinant CYP3A4 and HLMs. A) Extracts from $25OHD_3$ incubation with recombinant CYP3A4; B) seven authentic vitamin D_3 metabolites; C) extracts from $25OHD_3$ incubation with HLMs. M1 and M2 denote two major unknown metabolites.

Figure 2. Electron impact mass spectra of the trimethylsilyl ether derivatives of the two unknown metabolites M1 (A) and M2 (B). The metabolites were isolated and purified by HPLC before GC-MS analysis.

Figure 3. Identification of M1 and M2 by ^{1}H-NMR as 4-hydroxylated $25OHD_3$ metabolites. The chemical shifts of protons at C-6 and C-7 for $25OHD_3$, $1\alpha,25(OH)_2D_3$, M1 and M2 were assigned according to literature values (Eguchi and Ikekawa, 1990; Kamao et al., 2004).

Figure 4. Metabolism of $25OHD_3$ in primary human hepatocytes. Cells were treated with rifampin (RIF, 10 μM) or vehicle (0.1% DMSO) for 48 h, and then pre-incubated with DHB (20 μM) or vehicle (0.1% EtOH) to block CYP3A4 activity. Experimental details are under Experimental Procedures. The culture medium was collected and pooled for LC-MS/MS analysis.

Figure 5. Detection of $4\beta,25(OH)_2D_3$ in human plasma. A) LC-MS/MS-based ion current chromatograms of native plasma, and native plasma spiked with isolated $4\beta,25(OH)_2D_3$ (50 pg and 100 pg). B) Ion current chromatograms of HPLC-isolated fractions from native plasma (350

Molecular Pharmacology Fast Forward. Published on December 28, 2011 as DOI: 10.1124/mol.111.076356
This article has not been copyedited and formatted. The final version may differ from this version.

ml) and 4β,25$(OH)_2D_3$ standard. MRM was carried out by monitoring the transition *m/z* 574 → 314.

Figure 6. Correlation between rates of 4-hydroxylation of 25OHD_3 and CYP3A4 activity/content in HLMs from different liver tissues (n = 42). CYP3A4 activity was expressed as the sum of 1′- and 4-hydroxylation of midazolam (MDZ) and content was determined by Western blot (Lin et al., 2002).

Figure 7. Effect of short-term rifampin treatment (600 mg. once a day, for 7 days) on the plasma concentrations of dihydroxyvitamin D metabolites (A) and the metabolite to 25OHD_3 concentration ratios (B). Individual mean concentrations and ratios at baseline (average of day 0 and day 1, pre-RIF) and after rifampin treatment (average of day 7 and day 8, post-RIF) from six subjects are shown. Bars indicate the mean value for the group. The p value was calculated by paired t-test. NS: not significant.

Figure 8. Effect of short-term rifampin treatment on individual serum and urine levels of calcium and phosphate. A) serum calcium, B) serum phosphate, C) creatinine-normalized calcium (UCa/UCr × 1000) in spot urine and D) creatinine-normalized phosphate (UPi/UCr × 1000) in spot urine were measured in six subjects at baseline and after rifampin treatment. For each subject, the averages of two pre-rifampin measurements (day 0 and day 1) and two post-rifampin measurements (day 7 and day 8) are plotted. NS: not significant.

Molecular Pharmacology Fast Forward. Published on December 28, 2011 as DOI: 10.1124/mol.111.076356
This article has not been copyedited and formatted. The final version may differ from this version.

Figure 9. Correlation between absolute changes in plasma 4β,25$(OH)_2D_3$ concentration with absolute changes in the plasma 1α,25$(OH)_2D_3$ level (A) and urinary phosphate excretion (B) from six subjects. The absolute concentration change was calculated as the post-rifampin minus pre-rifampin concentrations. Sample correlation coefficients and corresponding p-values were calculated; the null hypothesis that the population correlation is zero was tested with a t-test, under the assumption that the population was bivariate normally distributed.

Figure 10. Proposed metabolic profile of 25OHD_3 by recombinant CYP3A4 *in vitro*. The relative percentage of metabolite/25OHD_3 was estimated using HPLC-UV assuming that each metabolite has the same UV absorption extinction coefficient at 265 nm. In vitro incubation conditions were described in "Experimental Procedures".

Molecular Pharmacology Fast Forward. Published on December 28, 2011 as DOI: 10.1124/mol.111.076356
This article has not been copyedited and formatted. The final version may differ from this version.

Table 1. Identification of dihydroxyvitamin D_3 metabolites by HPLC-UV, periodate cleavage and LC-MS/MS analysis. After incubation of $25OHD_3$ with recombinant CYP3A4 or HLM, the vitamin D_3 metabolites were extracted by LLE and reconstituted in mobile phase for HPLC-UV analysis. The fractions corresponding to eight peaks were collected, dried and subjected to PTAD derivatization. The derivatives were then divided into two parts, one for LC-MS/MS analysis directly and the other for periodate cleavage followed by LC-MS/MS analysis. The results were compared with those of authentic standards which were conducted under the same conditions.

Vitamin D metabolites	HPLC-UV[a]	LC-MS/MS after PTAD derivatization[a]		Periodate cleavage[b]	Assigned structures
	RT (min)	MRM (m/z)	RT (min)	Vicinal – OH groups?	
Peak 1	27.36	574 → 298	8.61;10.18	Yes	24S,25$(OH)_2D_3$
Peak 2	27.81	574 → 298	8.56; 10.13	Yes	24R,25$(OH)_2D_3$
Peak 3	28.61	574 → 298	8.59; 9.97	No	23S,25$(OH)_2D_3$
Peak 4	31.95	574 → 298	8.78; 9.81	Yes	25,26$(OH)_2D_3$
Peak 5	32.62	574 → 314	11.31; 12.15	Yes	4β,25$(OH)_2D_3$ (M1)
Peak 6	34.01	574 → 314	11.15; 11.91	Yes	4α,25$(OH)_2D_3$ (M2)
Peak 7	34.70	574 → 298	11.37	No	23R,25$(OH)_2D_3$
		574 → 314	11.62	No	1α,25$(OH)_2D_3$
		574 → 314	12.36	No	1α,25$(OH)_2$-3-epi-D_3
Peak 8	35.21	574 → 314	12.37	No	1α,25$(OH)_2$-3-epi-D_3
		574 → 314	11.62	No	1α,25$(OH)_2D_3$

[a] HPLC analysis was performed using Method I and LC-MS/MS analysis was performed using Method II. Experimental details are described under Experimental Procedures.
[b] After reaction with $NaIO_4$ or water as vehicle, metabolites were extracted by ethyl acetate; after evaporation, samples were reconstituted in acetonitrile (40%) for LC-MS/MS analysis.

Molecular Pharmacology Fast Forward. Published on December 28, 2011 as DOI: 10.1124/mol.111.076356
This article has not been copyedited and formatted. The final version may differ from this version.

Table 2. $25OHD_3$ 4-hydroxylase activity for various recombinant P450 enzymes. Incubations were carried out with 10 pmol of enzyme for 30 min. The metabolite formation rates for CYP3A4 and CYP3A5 were obtained from triplicate incubations for 10 min. Substrate $25OHD_3$ concentration was 12.5 μM.

P450s	Metabolite formation rate		
	24R,25$(OH)_2D_3$	4β,25$(OH)_2D_3$	4α,25$(OH)_2D_3$
	pmol/min/pmol	*pmol/min/pmol*	*pmol/min/pmol*
CYP3A4 (b_5 co-expressed)	BLQ[c]	2.27 ± 0.22	1.26 ± 0.27
CYP3A5 (b_5 co-expressed)	BLQ	0.24 ± 0.03	0.17 ± 0.02
CYP24A1[a]	2.39 ± 0.63	ND	ND
Other P450s[b]	ND[c]	ND	ND

[a] Metabolism of $25OHD_3$ by CYP24A1 was conducted in Dr. Sakaki's lab (Toyama Prefectural University, Japan). Incubation conditions: CYP24A1 (20 nM), adrenodoxin (ADX, 200 nM), adrenodoxin reductase (ADR, 20 nM), 1 mM NADPH and 12.5 μM $25OHD_3$ in 100 mM Tris-HCl (pH 7.4, 1mM EDTA) at 37 ^oC for 10 min. After incubation, the products were extracted and shipped to University of Washington. LC-MS/MS analysis was performed as described in "Materials and Methods".
[b] Other P450s: CYP1A1, 1A2, 2A6, 2B6, 2C8, 2C9, 2C19, 2D6, 2E1, 2J2 and 3A7.
[c] BLQ: below limit of quantification; ND: not detected.

Molecular Pharmacology Fast Forward. Published on December 28, 2011 as DOI: 10.1124/mol.111.076356
This article has not been copyedited and formatted. The final version may differ from this version.

Table 3. Kinetic parameters for the 4-hydroxylation of 25OHD$_3$ by recombinant CYP3A4 and HLMs. Values represent mean ± S.D. for triplicate incubations. Total intrinsic clearance (CL) is the sum of V_{max}/K_m for these two major products [4β,25(OH)$_2$D$_3$ and 4α,25(OH)$_2$D$_3$].

	4β,25(OH)$_2$D$_3$		4α,25(OH)$_2$D$_3$		Total Intrinsic CL
	V_{max}	K_m	V_{max}	K_m	V_{max}/K_m
	pmol/min/pmol	*μM*	*pmol/min/pmol*	*μM*	*ml/min/nmol*
CYP3A4 (b_5 co-expressed)	6.4 ± 0.99	7.5 ± 1.35	3.0 ± 0.25	6.4 ± 0.86	1.32
HLMs[a]	229 ± 62.7	18.8 ± 4.6	105 ± 13.8	13.3 ± 1.8	0.22[b]

[a] V_{max} is expressed as picomoles per minute per milligram of protein.
[b] Calculated based on the CYP3A4 protein level as determined by western blot (Lin et al., 2002).

Molecular Pharmacology Fast Forward. Published on December 28, 2011 as DOI: 10.1124/mol.111.076356
This article has not been copyedited and formatted. The final version may differ from this version.

Table 4. Inhibition of $25OHD_3$ 4-hydroxylation activity by CYP3A4 and HLMs by 6′,7′-dihydroxybergamottin (DHB) and ketoconazole (KTZ). Experimental details are described under Materials and Methods.

	Recombinant CYP3A4		Human Liver Microsomes	
	$4\beta,25(OH)_2D_3$	$4\alpha,25(OH)_2D_3$	$4\beta,25(OH)_2D_3$	$4\alpha,25(OH)_2D_3$
	% of control		% of control	
DHB	0.34 ± 0.04	0.77 ± 0.19	2.61 ± 0.61	2.90 ± 0.04
KTZ	17.6 ± 3.38	18.5 ± 2.28	11.0 ± 1.82	18.5 ± 5.61

Figure 1

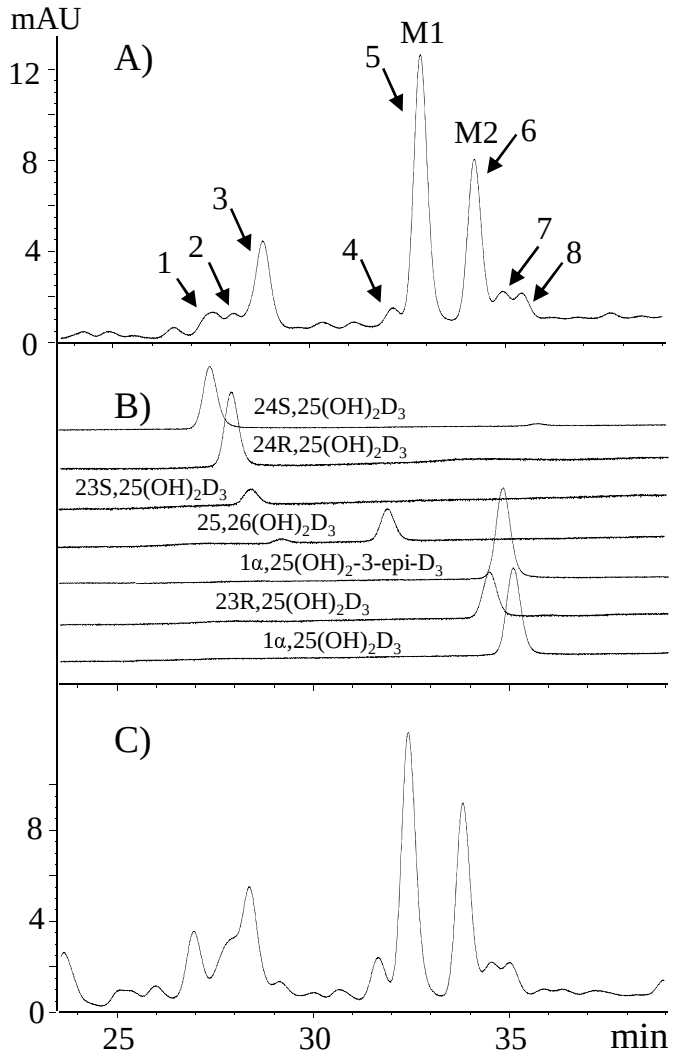

Figure 2

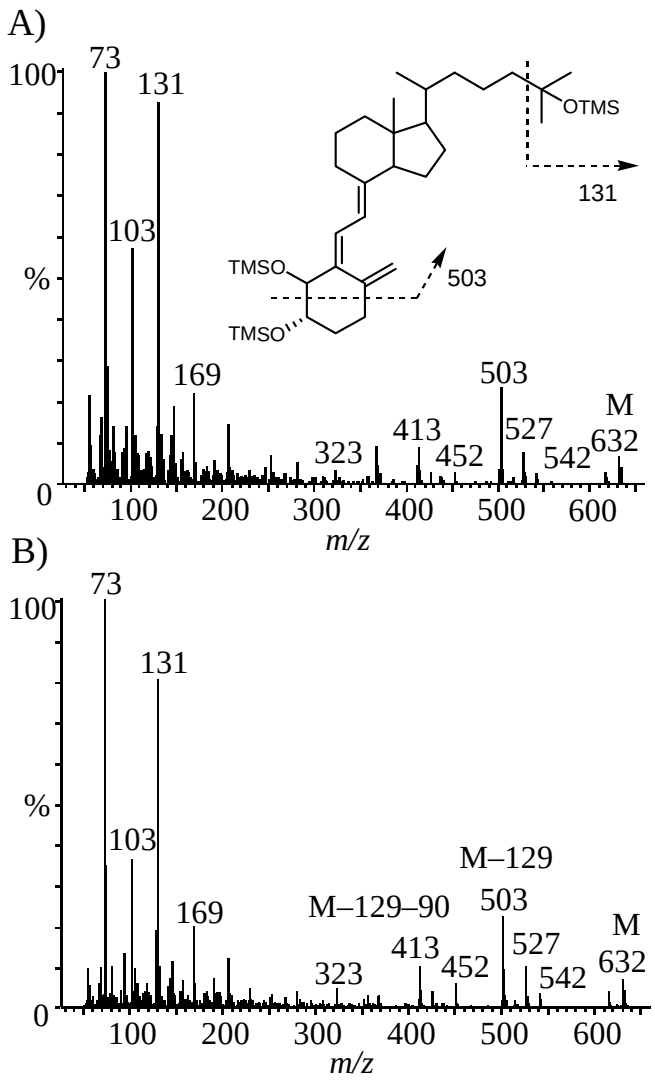

Figure 3

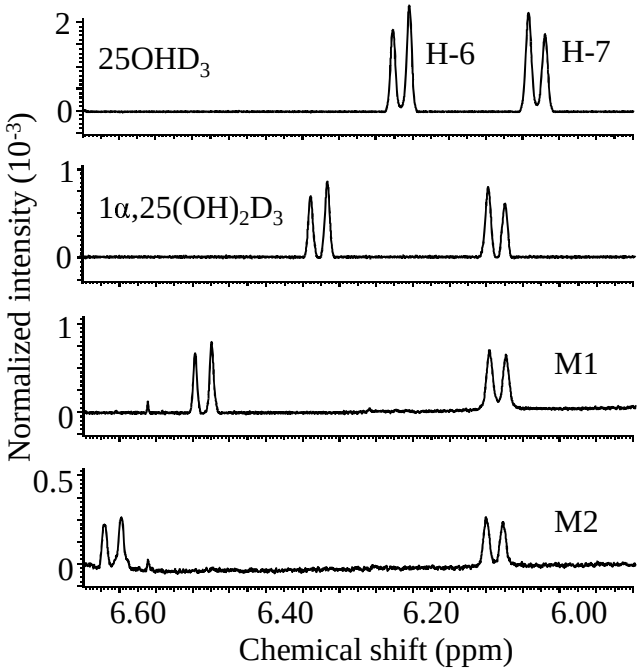

Figure 4

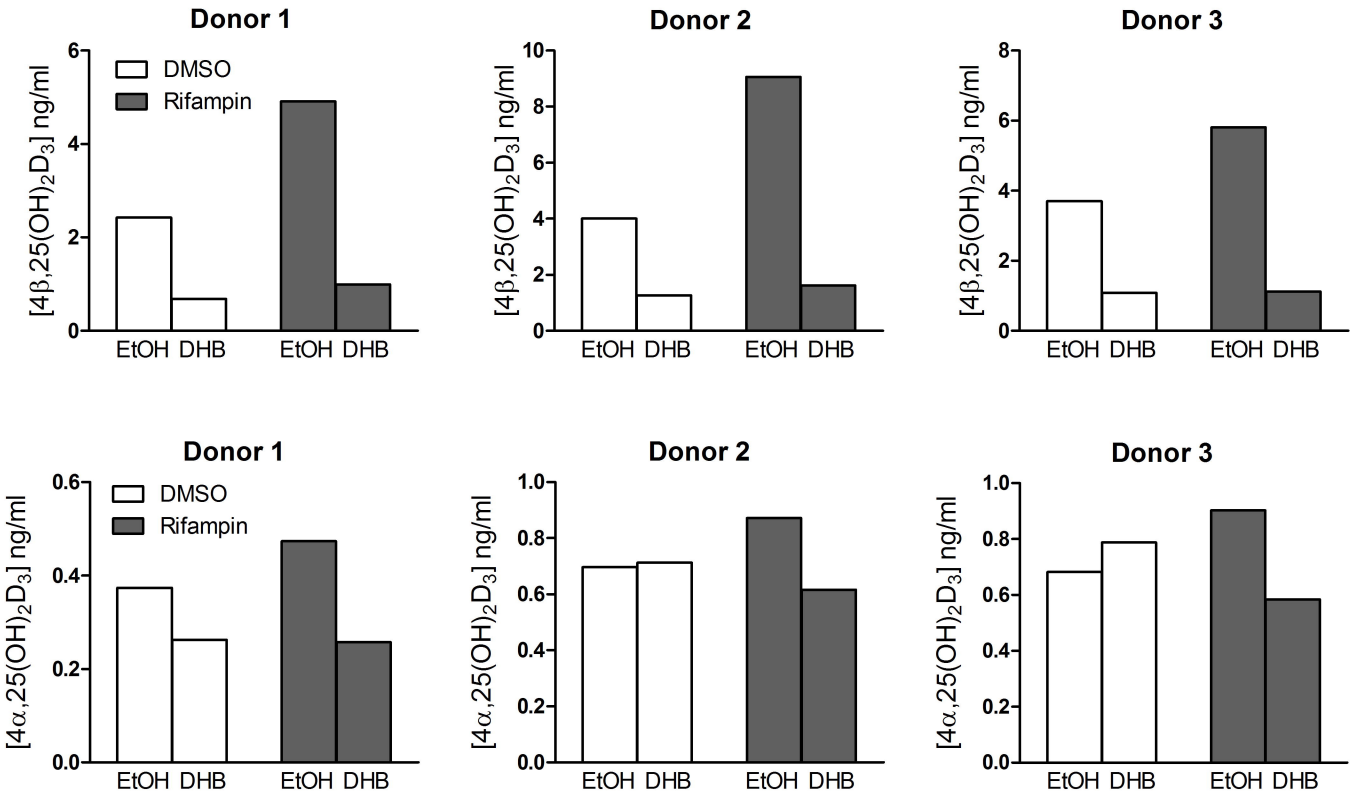
Donor 1
DMSO
Rifampin
[4β,25(OH)2D3] ng/ml
0
2
4
6
EtOH DHB EtOH DHB
Donor 2
[4β,25(OH)2D3] ng/ml
0
2
4
6
8
10
EtOH DHB EtOH DHB
Donor 3
[4β,25(OH)2D3] ng/ml
0
2
4
6
8
EtOH DHB EtOH DHB
Donor 1
DMSO
Rifampin
[4α,25(OH)2D3] ng/ml
0.0
0.2
0.4
0.6
EtOH DHB EtOH DHB
Donor 2
[4α,25(OH)2D3] ng/ml
0.0
0.2
0.4
0.6
0.8
1.0
EtOH DHB EtOH DHB
Donor 3
[4α,25(OH)2D3] ng/ml
0.0
0.2
0.4
0.6
0.8
1.0
EtOH DHB EtOH DHB

Figure 5

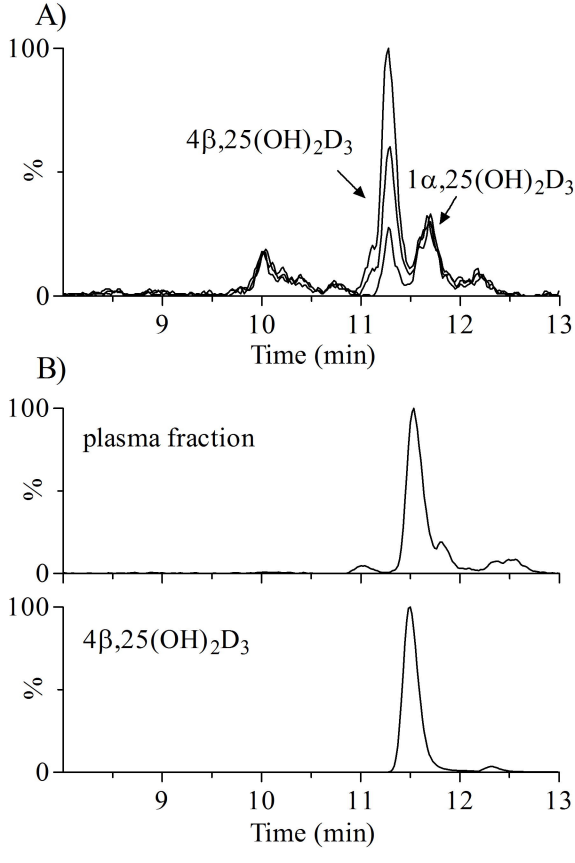
A)
100
%
0
4β,25(OH)2D3
1α,25(OH)2D3
9
10
11
12
13
Time (min)
B)
100
%
0
plasma fraction
100
%
0
4β,25(OH)2D3
9
10
11
12
13
Time (min)

Figure 6

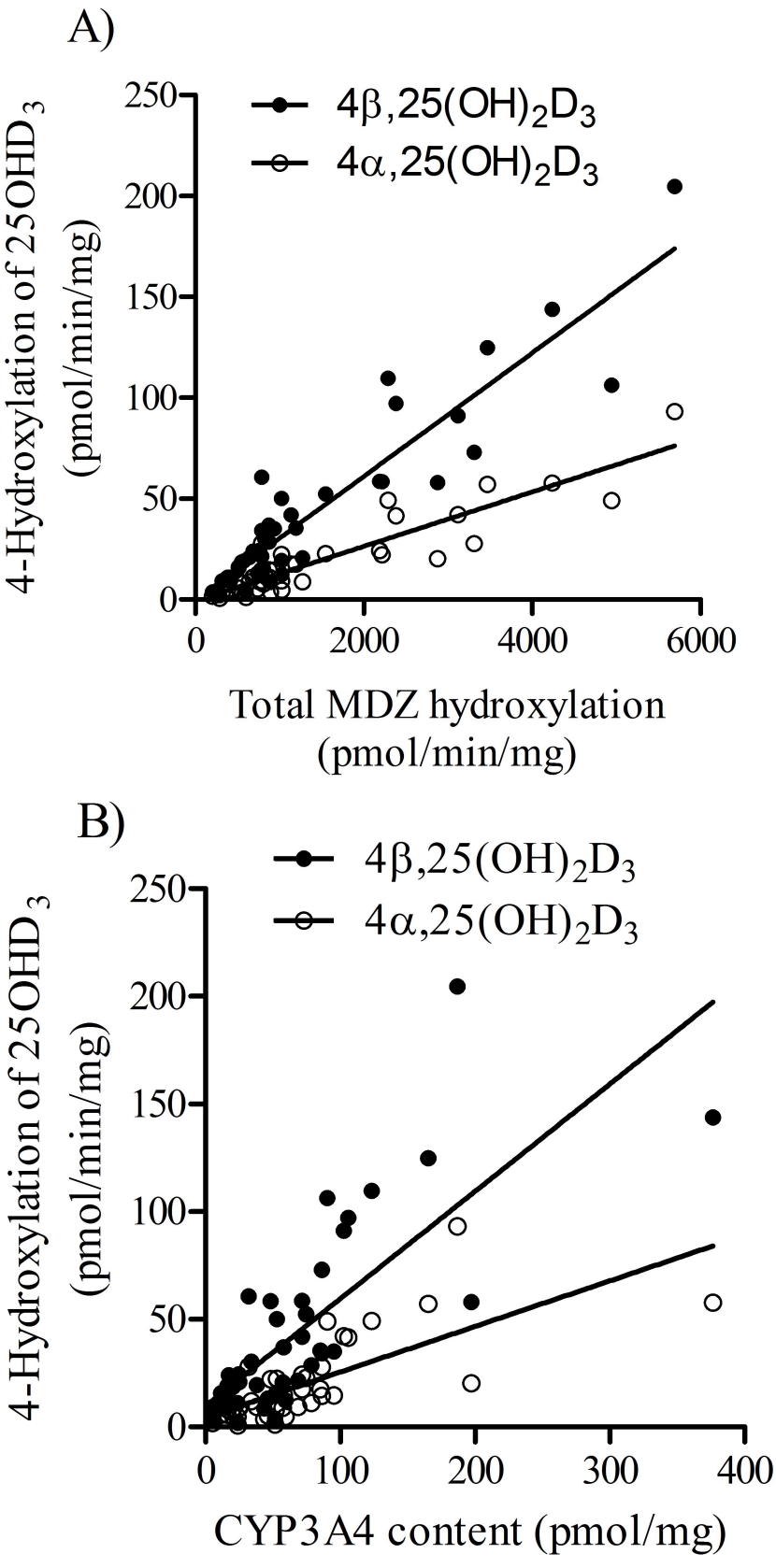
A)
4β,25(OH)2D3
4α,25(OH)2D3
4-Hydroxylation of 25OHD3 (pmol/min/mg)
250
200
150
100
50
0
0
2000
4000
6000
Total MDZ hydroxylation (pmol/min/mg)
B)
4β,25(OH)2D3
4α,25(OH)2D3
4-Hydroxylation of 25OHD3 (pmol/min/mg)
250
200
150
100
50
0
0
100
200
300
400
CYP3A4 content (pmol/mg)

Figure 7

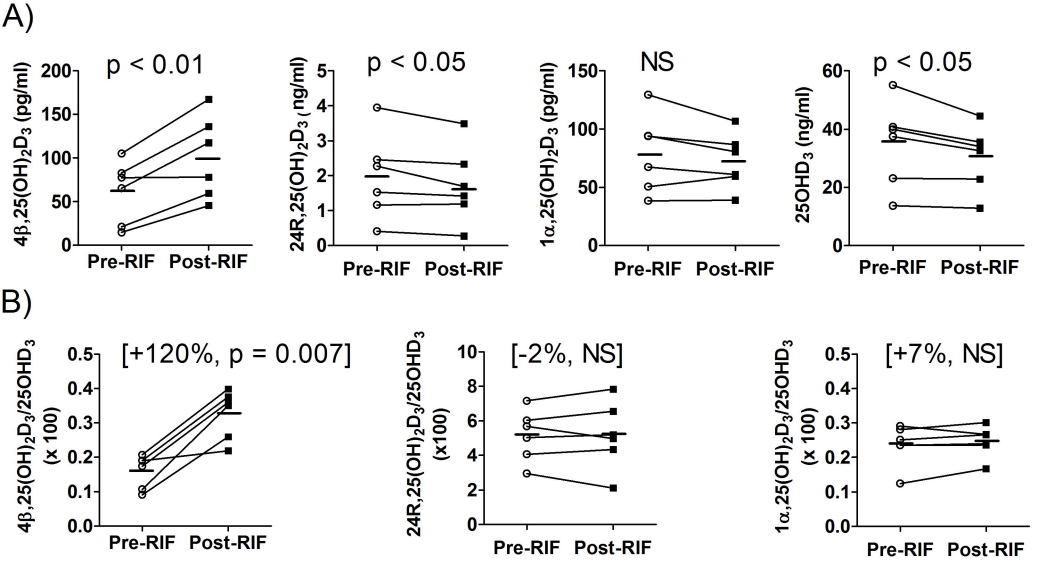
A)
p < 0.01
4β,25(OH)2D3 (pg/ml)
200
150
100
50
0
Pre-RIF
Post-RIF
p < 0.05
24R,25(OH)2D3 (ng/ml)
5
4
3
2
1
0
Pre-RIF
Post-RIF
NS
1α,25(OH)2D3 (pg/ml)
150
100
50
0
Pre-RIF
Post-RIF
p < 0.05
25OHD3 (ng/ml)
60
40
20
0
Pre-RIF
Post-RIF
B)
[+120%, p = 0.007]
4β,25(OH)2D3/25OHD3 (x 100)
0.5
0.4
0.3
0.2
0.1
0.0
Pre-RIF
Post-RIF
[-2%, NS]
24R,25(OH)2D3/25OHD3 (x100)
10
8
6
4
2
0
Pre-RIF
Post-RIF
[+7%, NS]
1α,25(OH)2D3/25OHD3 (x 100)
0.5
0.4
0.3
0.2
0.1
0.0
Pre-RIF
Post-RIF

Figure 8

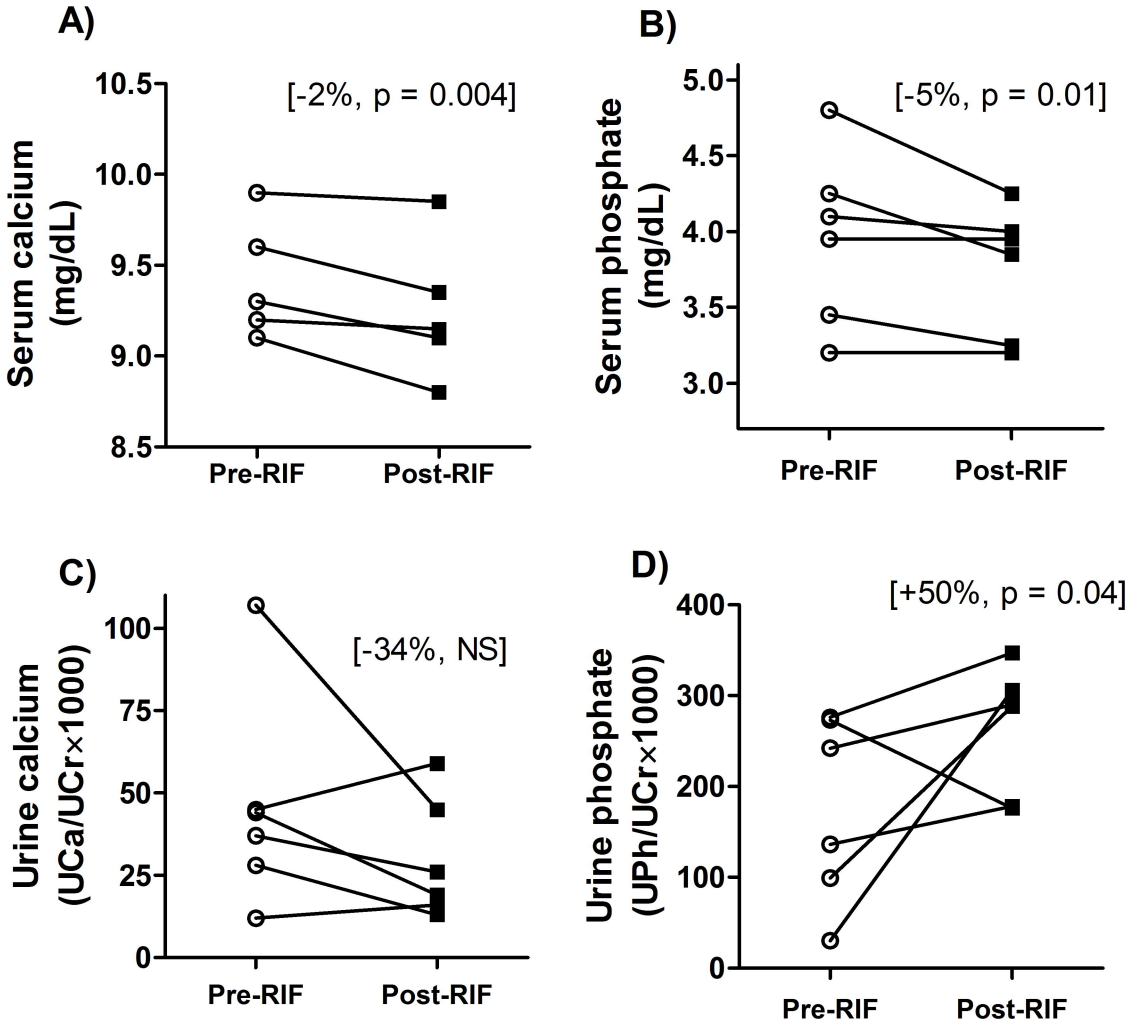
A)
Serum calcium (mg/dL)
10.5
10.0
9.5
9.0
8.5
[-2%, p = 0.004]
Pre-RIF
Post-RIF
B)
Serum phosphate (mg/dL)
5.0
4.5
4.0
3.5
3.0
[-5%, p = 0.01]
Pre-RIF
Post-RIF
C)
Urine calcium (UCa/UCr×1000)
100
75
50
25
0
[-34%, NS]
Pre-RIF
Post-RIF
D)
Urine phosphate (UPh/UCr×1000)
400
300
200
100
0
[+50%, p = 0.04]
Pre-RIF
Post-RIF

Figure 9

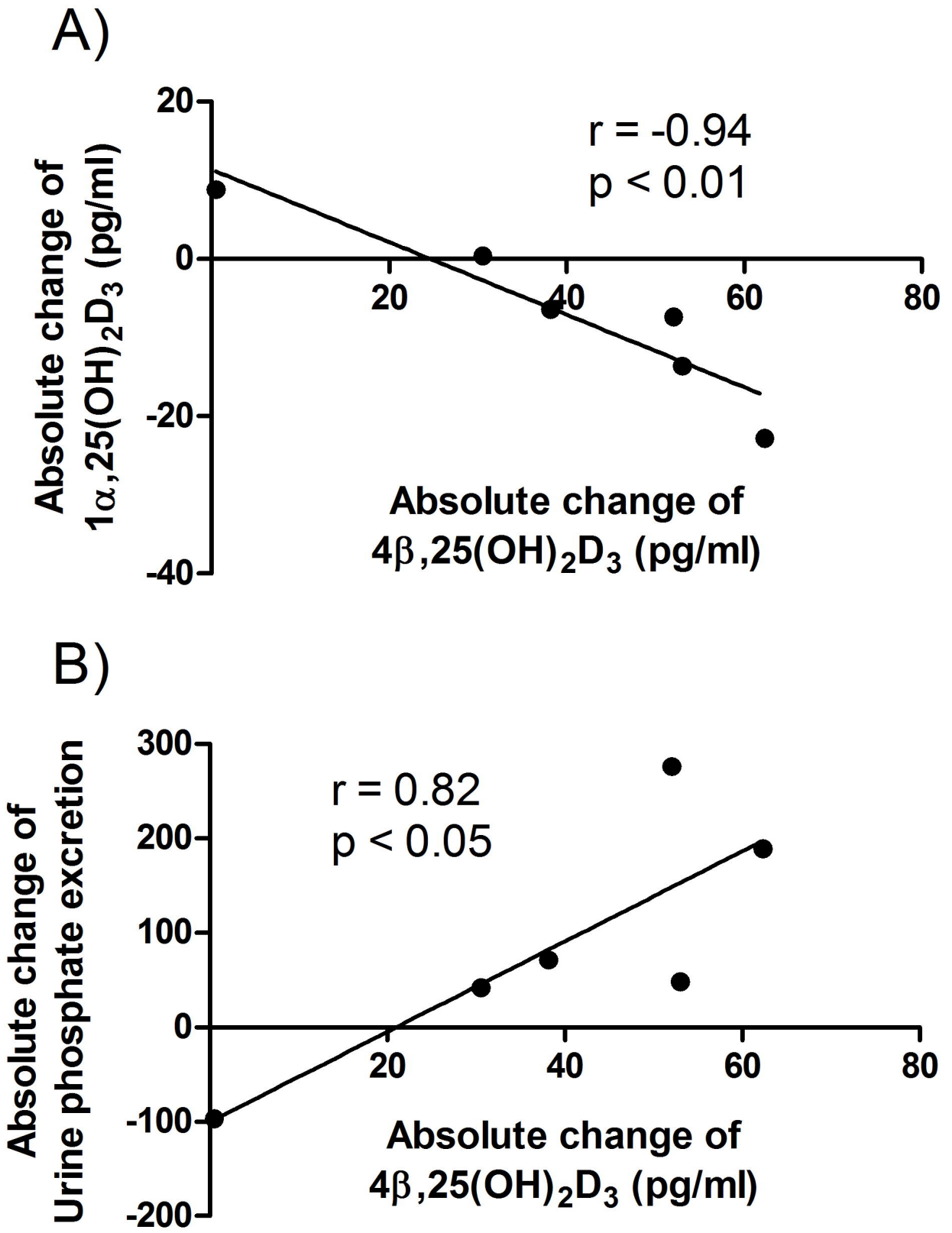
A)
20
0
-20
-40
20
40
60
80
r = -0.94
p < 0.01
Absolute change of
1α,25(OH)2D3 (pg/ml)
Absolute change of
4β,25(OH)2D3 (pg/ml)
B)
300
200
100
0
-100
-200
20
40
60
80
r = 0.82
p < 0.05
Absolute change of
Urine phosphate excretion
Absolute change of
4β,25(OH)2D3 (pg/ml)

Figure 10